

# The effect of plasmin-mediated degradation on fibrinolysis and tissue plasminogen activator diffusion

Brittany E. Bannish,<sup>1,\*</sup> Bradley Paynter,<sup>1</sup> Rebecca A. Risman,<sup>2</sup> Mitali Shroff,<sup>3</sup> and Valerie Tutowler<sup>2,\*</sup>

<sup>1</sup>University of Central Oklahoma, Department of Mathematics and Statistics, Edmond, Oklahoma; <sup>2</sup>Rutgers University, Department of Biomedical Engineering, Piscataway, New Jersey; and <sup>3</sup>Rutgers University, Department of Cell Biology and Neuroscience, Piscataway, New Jersey

**ABSTRACT** We modify a three-dimensional multiscale model of fibrinolysis to study the effect of plasmin-mediated degradation of fibrin on tissue plasminogen activator (tPA) diffusion and fibrinolysis. We propose that tPA is released from a fibrin fiber by simple kinetic unbinding, as well as by “forced unbinding,” which occurs when plasmin degrades fibrin to which tPA is bound. We show that, if tPA is bound to a small-enough piece of fibrin that it can diffuse *into* the clot, then plasmin can *increase* the effective diffusion of tPA. If tPA is bound to larger fibrin degradation products (FDPs) that can only diffuse *along* the clot, then plasmin can *decrease* the effective diffusion of tPA. We find that lysis rates are fastest when tPA is bound to fibrin that can diffuse into the clot, and slowest when tPA is bound to FDPs that can only diffuse along the clot. Laboratory experiments confirm that FDPs can diffuse into a clot, and they support the model hypothesis that forced unbinding of tPA results in a mix of FDPs, such that tPA bound to FDPs can diffuse both into and along the clot. Regardless of how tPA is released from a fiber, a tPA mutant with a smaller dissociation constant results in slower lysis (because tPA binds strongly to fibrin), and a tPA mutant with a larger dissociation constant results in faster lysis.

**SIGNIFICANCE** Blood clots are critical to prevent bleeding, but serious complications such as stroke can occur if clots are not enzymatically degraded effectively via fibrinolysis. This work proposes a novel mechanism for the regulation of fibrinolysis: forced unbinding of tissue plasminogen activator (tPA) by plasmin-mediated degradation of fibrin. This forced unbinding of tPA can influence the effective diffusion of tPA through the clot and the clot lysis rate. Depending on the situation, plasmin hinders or enhances tPA effective diffusion. Understanding the role of forced unbinding during lysis aids in development of novel therapeutics to treat stroke.

## INTRODUCTION

Blood clots are composed of red blood cells, platelets, and a mesh of fibrin fibers that stabilizes the clot. Fibrinolysis is the natural, enzymatic degradation of this fibrin mesh. A fibrin monomer consists of three pairs of polypeptide chains— $\alpha$ ,  $\beta$ , and  $\gamma$ —held together by disulfide bonds (1). Two strands of fibrin monomers aggregate in a half-staggered manner to form a protofibril (2). Protomembranes laterally aggregate into fibrin fibers, which form the fibrin network. During fibrinolysis, tissue plasminogen activator (tPA) binds to fibrin fibers and activates bound plasminogen to

plasmin. Plasmin degrades fibrin, producing soluble fibrin degradation products (FDPs) (3,4), which can be removed from the clot via diffusion and blood flow, leading to the dissolution of the clot matrix.

When the natural process of fibrinolysis does not work appropriately, dangerous blood clots may form, resulting in life- and limb-threatening complications. For example, when a blood vessel in the brain is blocked by a blood clot, ischemic stroke may result. Stroke is one of the leading causes of death and disability worldwide (5). Thrombolysis is the clinical degradation of blood clots using “clot-busting” drugs such as recombinant tPA. Experiments that mimic thrombolysis by adding tPA to a preformed clot find that lysis proceeds as a front, with a high concentration of tPA at the front (6–8). Although recombinant tPA is the only Food and Drug Administration-approved thrombolytic

Submitted July 18, 2023, and accepted for publication February 2, 2024.

\*Correspondence: [bbannish@uco.edu](mailto:bbannish@uco.edu) or [vt280@soe.rutgers.edu](mailto:vt280@soe.rutgers.edu)

Editor: Tuomas Knowles.

<https://doi.org/10.1016/j.bpj.2024.02.002>

© 2024 Biophysical Society.

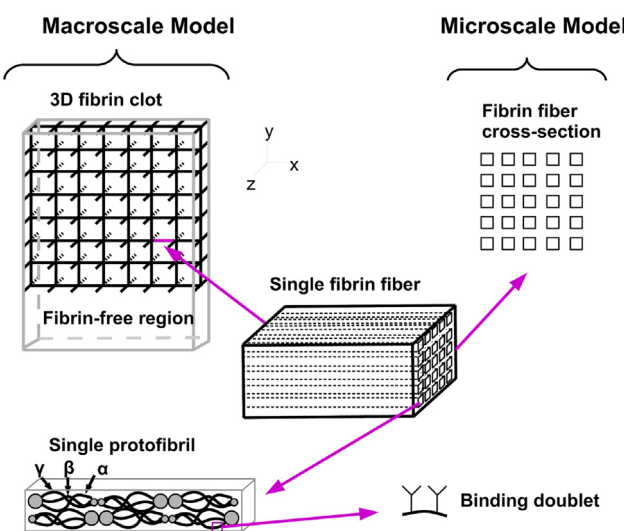


FIGURE 1 Multiscale model overview. The macroscale model is a 3D square lattice one edge deep in the direction coming out of the page. Each lattice edge represents a fibrin fiber. There is a fibrin-free region abutting the clot where tPA is added to initiate lysis. Biologically, a single fibrin fiber is composed of bundles of protofibrils. A protofibril is a chain of half-staggered fibrin monomers, each of which contains an  $\alpha$ ,  $\beta$ , and  $\gamma$  chain. Binding sites for tPA, plasminogen, and plasmin are located on these chains. For simplicity, we approximate the roughly cylindrical fibrin fibers and protofibrils by rectangular boxes of equal volume, and we assume that the protofibrils are spaced out evenly within the fiber volume. The microscale model is a 2D fiber cross section (*upper right of figure*). The boxes represent the cross sections of the protofibrils, and we assume that each protofibril cross section contains six “binding doublets”—pairs of binding sites for the fibrinolytic enzymes—corresponding to binding sites on the six chains (two each of  $\alpha$ ,  $\beta$ , and  $\gamma$ ) of the half-staggered fibrin monomers.

for ischemic stroke (9), its efficacy and safety are concerns (10,11). Much laboratory work has been done to create tPA variants that have a longer half-life, are more resistant to inhibitors, and have a stronger binding affinity for fibrin (12,13). Most of these studies looked at myocardial infarction (not ischemic stroke) and assumed that high fibrin binding affinity is an important feature of the tPA variant. However, one tPA mutant, reteplase, has a weaker binding affinity and improved fibrinolytic efficacy (12,14). Thrombolytic therapies use intravenous tPA, which initiates the creation of plasmin on fibrin fibers, rather than plasmin directly to avoid strong plasmin inhibitors that circulate naturally in the blood (15). Ultimately, though, it is plasmin that degrades the fibrin.

Depending on the relative locations of the plasmin-mediated cleavages of fibrin, various soluble FDPs can be produced that still contain binding sites attractive to tPA. These FDPs have weight-averaged molar masses ranging from 250 to 10,000 kDa and an approximate root-mean-square radius ranging from 12 to 85 nm (16). This corresponds to pieces the size of one fibrin monomer, up to the size of 40 connected monomers. Experimental data show that smaller FDPs perfuse through the clot at a higher rate than large FDPs even though they should be created in

approximately equal amounts (16). It is hypothesized that this is due to FDPs binding to the remaining clot with an affinity proportional to their size. These differences can influence the distribution of bound tPA throughout the clot. For example, tPA could be physically removed from the clot or brought deeper into the clot, due to being bound to a small FDP that is able to freely diffuse everywhere. Alternatively, tPA could be held in place, being bound to a large FDP that is stuck to the remaining clot. It is unknown how much tPA is sequestered on FDPs, unable to bind to other fibers and initiate degradation. Additionally, it is unknown exactly how tPA is affected by plasmin-mediated degradation of fibrin.

This paper aims to use mathematical modeling supported by laboratory experimentation to better understand the physiological mechanisms behind tPA-induced fibrinolysis and thrombolysis and to suggest targets for thrombolytic drug development. In particular, we are interested in the effect of plasmin-mediated fibrin degradation on the effective diffusion of tPA through a clot, and consequently on the rate of fibrinolysis. We consider four possible mechanisms of how tPA is affected by plasmin, and we consider also how tPA variants might be exploited for improved therapeutic outcomes.

## MATERIALS AND METHODS

We started with the multiscale model of Bannish et al. (17) and modified it to study the different possible mechanisms of tPA unbinding and diffusion. This model consists of a two-dimensional (2D) microscale model of a fiber cross section coupled to a three-dimensional (3D) macroscale model of a fibrin clot (Fig. 1). For a more detailed explanation of the model, see (17,18). The model is summarized briefly below. Simulations were run using a custom Fortran code with Python used to dispatch simulations, collate data, and post-process results.

## Microscale model

The microscale model of a fiber cross section is represented by a 2D arrangement of protofibril cross sections, each of which contains binding doublets (Fig. 1) to which tPA, plasminogen, and plasmin can bind and that can be degraded by plasmin. Plasminogen is present throughout the cross section, and the model is initialized by randomly placing a single tPA molecule on the outer edge of the fiber. This tPA molecule can activate plasminogen to plasmin, which can crawl to neighboring binding doublets, degrade fibrin, or unbind from fibrin completely. The protofibril cross sections in the microscale model are spaced out similarly to actual protofibrils. Each protofibril cross section has six binding doublets that must be cleaved by plasmin for total degradation of that protofibril. These six doublets correspond to the six chains (two each of  $\alpha$ ,  $\beta$ , and  $\gamma$ ) of the half-staggered fibrin monomers. The single fibrin fiber is considered to be degraded when two-thirds of the binding doublets within the cross section have been cleaved by plasmin. When tPA unbinds from the microscale model, it is removed from the simulation, because the probability that the molecule would rebind to the exact same cross section of the fiber is so small (18). We use the Gillespie algorithm (19,20) to determine which reaction happens and the time at which it occurs. Due to the stochasticity of the microscale model, we run the model 50,000 independent times. The outcomes of these simulations form empirical distributions of the single-fiber lysis time (how long it takes

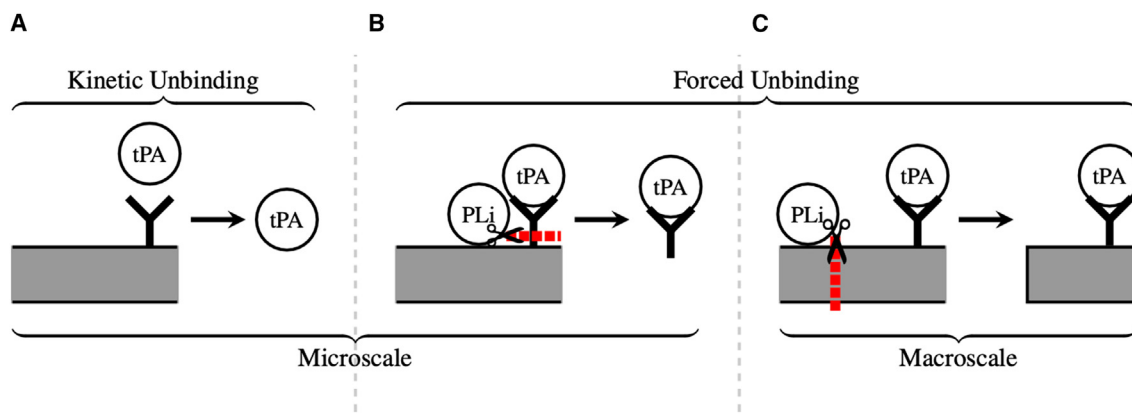


FIGURE 2 Three possible mechanisms for the unbinding of tPA. (A) tPA kinetically unbinds from fibrin and may diffuse or bind on another fiber. (B) Plasmin (PLi)-mediated degradation, represented by red lines, releases tPA that is bound to a small piece of fibrin (the “Y” shape), whose ability to diffuse may be restricted, and the tPA is unable to bind to another fiber. (C) Plasmin-mediated degradation, represented by red lines, releases tPA that is bound to a large FDP, whose ability to diffuse may be restricted, and the tPA is unable to bind to another fiber. In both mechanisms (B) and (C), which we term “forced unbinding,” the tPA molecule will eventually kinetically unbind from the piece of fibrin to which it is bound, at which point it will be able to bind to another fiber.

one fibrin fiber to be cut by plasmin) and the tPA leaving time (the time at which tPA left the particular cross section).

### Macroscale model and linking the scales

The macroscale model is a 3D square lattice with each lattice edge representing a fibrin fiber. Each fibrin fiber has a diameter of 72.7 nm, and the pore size between fibers is 1.0135  $\mu\text{m}$ , both of which are in the range of physiological values (21,22). A bolus of tPA is added to the fibrin-free region abutting the clot, and tPA is allowed to diffuse, bind to fibers, and unbind from fibers. The location and bound/unbound status of every tPA molecule is tracked at every step of the algorithm (time step =  $0.3424\text{e-}04$  s), as is the degradation status of every fiber in the clot. When a tPA molecule binds to a fiber, we randomly sample the empirical distributions of lysis time and tPA leaving time to determine if/when the fiber degrades and when that particular tPA molecule will unbind.

For each set of model experimental conditions, we run 10 independent simulations of the macroscale model. Each simulation is run until all fibers are degraded and at least 95% of molecules have reached the back row of the clot. The status of the model is recorded at 10-s intervals, which we found to be short enough to capture dynamics and long enough to avoid generating datasets too unwieldy for postprocessing and storage. To measure the nature of the lysis process in the macroscale model, we calculate the lysis front velocity and first-passage time of tPA to reach the back of the clot. To calculate the lysis front velocity, we track the lowest y-position of the fibrin clot at each data record at each x-location of the lattice. A linear least-squares fit is made for this position over time, and the slope of that fit is taken as the velocity for that location in  $\mu\text{m}/\text{min}$ . To calculate the first-passage time of tPA, we record the first time each individual tPA molecule reaches a fiber on the back edge of the clot (farthest from where tPA was introduced in the fibrin-free region). We also tally the number of tPA unbinding events of each type (more on this below) for each simulation. It should be noted that, due to the way molecules are tracked in the macroscale model, in any simulation, the number of times a molecule binds is exactly the same as the number of times that same molecule unbinds. A table of macroscale model parameters is provided in Table S1.

### tPA unbinding mechanisms

Since the mechanisms by which tPA is affected by plasmin-mediated degradation of fibrin are unknown, we investigate plausible candidates using the

multiscale model. In the model, there are three mechanisms by which a tPA molecule is removed from a fiber: 1) the molecule can kinetically unbind from its binding site and drift out of the cross section (Fig. 2 A). This occurs in the microscale model. 2) The binding site to which the molecule is bound can be degraded by plasmin, leading to its removal from the cross section (Fig. 2 B). This also occurs in the microscale and is the first case of what we term “forced” unbinding. (3) The fiber to which the molecule is bound is degraded as a result of the action of plasmin in a separate cross section, activated by a separate tPA molecule (Fig. 2 C). This occurs in the macroscale model and is the second case of forced unbinding. Earlier macroscale models (17,18) did not distinguish between kinetic and forced unbinding of tPA; tPA was always immediately free to diffuse through the clot and available to rebind to fibrin, whether it kinetically unbound or was forced to unbind by plasmin-mediated degradation of fibrin. In this paper, we study the more realistic mechanism in which tPA that is forced to unbind by plasmin remains bound to fibrin for some time (during which it is unable to rebinding to other fibrin and is possibly restricted in its movement) and then eventually kinetically unbinds and is able to rebinding elsewhere. Since the physiological details of forced unbinding are currently unknown, we use modeling to test the most likely mechanisms, described below. Note that, in all mechanisms, the moving and “rebinding” of tPA only happens on the macroscale, because the probability of rebinding to the same fiber cross section is so small that we assume tPA can never rebinding on the microscale. A summary of the unbinding mechanisms is provided in Table 1. Additional details about how the model treats diffusion of tPA and FDPs are provided in the Supporting Material.

#### Always rebind

In this mechanism, all tPA, regardless of how it was removed from the fiber on the microscale or macroscale, is immediately available for rebinding on the macroscale. This is how tPA was treated in previous models (17,18). In other words, tPA that kinetically unbinds is indistinguishable from tPA that is forced to unbind.

#### Diffuse into clot

In this mechanism, when tPA is forced to unbind on the microscale or macroscale, we imagine that it is still bound to a small piece of fibrin. We assume the piece of fibrin is small enough to diffuse freely throughout the clot. For all 50,000 microscale simulations, we record whether tPA

**TABLE 1 A summary of unbinding mechanisms and their restrictions in model variants**

Mechanism	Always rebind	Diffuse into clot	Diffuse along clot	Diffuse into and along clot
Kinetic	can bind immediately can move freely	can bind immediately can move freely	can bind immediately can move freely	can bind immediately can move freely
Forced (microscale)	can bind immediately can move freely	must wait to bind can move freely	must wait to bind must wait to move freely	must wait to bind can move freely
Forced (macroscale)	can bind immediately can move freely	must wait to bind can move freely	must wait to bind must wait to move freely	must wait to bind must wait to move freely

kinetically unbound, was forced to unbind, or remained bound for the entire simulation. Then we calculate the fraction of the simulations in which tPA was forced to unbind, given that it unbound, and consider this the “forced unbinding probability.” An example of these data is given in Fig. 3 C. At the macroscale, whenever tPA binds to a fiber, we randomly pick an unbinding time from the empirical distribution calculated from the microscale model (e.g., Fig. 3 A). After that length of time has passed, we pick another uniformly distributed random number. If that random number is less than the forced unbinding probability, then we consider that tPA molecule to be forcibly unbound from the fiber and bound to a small piece of fibrin that is able to freely diffuse. The tPA molecule continues to diffuse (with the small piece of fibrin) but is unable to bind to a new fiber until it kinetically unbinds from the small piece of fibrin. In this way, tPA is transported through the clot by “hitching a ride” on a small piece of fibrin. Similarly, tPA that is forced to unbind at the macroscale via degradation of the fibrin fiber to which it is bound is then assumed to be bound to a small piece of fibrin that can freely diffuse through the clot. When the decision is made to forcibly unbind a tPA molecule, we assign that molecule an average kinetic unbinding time ( $1/k_{off}$ ). After the average kinetic unbinding time has passed, the tPA molecule is released from the fibrin and is free to rebinding elsewhere.

### Diffuse along clot

This mechanism is almost identical to the case above, except that, when tPA is forced to unbind on the microscale or macroscale, we imagine that it is still bound to a large FDP, which is unable to diffuse through the clot but can diffuse along the face of the clot and away from the clot where there are no fibers to hinder the diffusion. The tPA molecule is only available to bind to a new fiber once it kinetically unbinds from the FDP.

### Diffuse into and along clot

In this mechanism, if tPA is forced to unbind on the microscale (i.e., if the random number is less than the forced unbinding probability, which we interpret as the binding doublet it was bound to degrading), then we imagine that the tPA is bound to a small piece of fibrin that is able to diffuse into the clot. If tPA is forced to unbind on the macroscale (i.e., if the fiber it was bound to degrades), then we imagine that it is bound to a large FDP that is only able to diffuse along or away from the clot. In both cases, tPA remains bound to the fibrin until it kinetically unbinds, at which point it is available to rebinding elsewhere.

### Confocal microscopy

To experimentally validate the model findings, we performed three sets of experiments using confocal microscopy (illustrated in Fig. S2). Commercially available human-pooled blood plasma (Cone Bioproducts #5781, fibrinogen concentration 2.9 mg/mL) was warmed to 37°C before all experiments. First, we tracked lysis of a fibrin clot over time with labeled fibrinogen and labeled tPA. A clot chamber was assembled with a glass slide and cover slip; layered double-sided tape was used to separate the glass pieces to create a channel. A plasma mixture (plasma with 1.2 mg/mL final fibrinogen concentration, 0.1 U/mL thrombin, 25 mM CaCl<sub>2</sub>, and 0.6% by vol-

ume Alexa 647 nm-labeled fibrinogen) was mixed, added to the chamber, and allowed to clot for at least 20 min at room temperature. Plasma was diluted with a buffer (50 mM Tris, 140 mM NaCl, 1 mg/mL bovine serum albumin) to achieve the final concentration. A tPA solution (77,000 ng/mL concentration, Alexa Fluorophore 488 nm) was carefully added to the chamber at the clot edge. Time-lapse images were captured every minute for 1 h at 10× and every 10 s for 10 min at 40× (water immersion) on a Zeiss LSM 800 confocal microscope (NA = 1.20, 1024 × 1024 pixels, scan rate of 3.78 s). Lysis front movement was measured as the distance the tPA “border” moved from the lysis front starting position since time at relative  $t = 0$  using the FIJI (Image J) line measuring tool. Measurements were taken at three locations per time lapse on three time lapses from three independent samples.

The second set of experiments utilized an alternative chamber to better visualize the movement of tPA along the fibrin edge vs. the movement of tPA into the clot. CoverWell perfusion chambers with the dimensions 6.35 × 19 × 2.5-mm depth were adhered to a glass slide (CoverWell™ Perfusion Chambers, Electron Microscopy Sciences, 70326-44). A plasma mix was made as described above and added to the chamber through one of the inlets. A tPA solution (77,000 ng/mL concentration) was added to the other inlet. An image was captured at this intersection at 40× magnification (water immersion) to qualitatively observe tPA interactions with the fibrin fibers.

For a third set of experiments to track movement of FDPs, a plasma mixture (plasma with 2.4 mg/mL fibrinogen, 75 pM tissue factor, 25 mM CaCl<sub>2</sub>, 1% by volume Alexa 594-labeled fibrinogen) was mixed, added to the chamber, and allowed to clot for 30 min. To correspond with the resulting images, we refer to this as the “top” clot. A second plasma mixture with a different fluorophore (plasma with 2.4 mg/mL fibrinogen, 0.5 U/mL thrombin, 25 mM CaCl<sub>2</sub>, 1% by volume Alexa 647-labeled fibrinogen) was mixed, added as a thin layer next to the top clot, and allowed to clot for 30 min. We refer to this as the “bottom” clot. A labeled tPA solution (Alexa 488, 77,000 ng/mL concentration) was carefully added to the chamber at the edge of the bottom clot. Timelapse images were captured every 30 s for 1 h on a Zeiss LSM 800 confocal microscope (NA = 1.20). After performing experiments with this two-clot system, we observed tPA, as well as portions of the bottom clot (magenta), diffusing into the top clot (blue) during lysis. To measure this observation, the channels were split, made binary, and the percentage area fraction of each channel in the region originally occupied by the first clot was measured on FIJI.

## RESULTS

### Microscale model

The base results of 50,000 independent simulations of the microscale model are presented in Fig. 3 labeled “Physiological  $K_d$ .”  $K_d$ , the dissociation constant for tPA binding to fibrin, is defined as the ratio of the unbinding rate to the binding rate:  $K_d = k_{off}/k_{on}$ . Using the physiological parameters in Table 2, on average, tPA stays bound to a given fiber cross section for just over 28 s (Fig. 3 A; Table S2), and a single fiber takes about 54 s to degrade

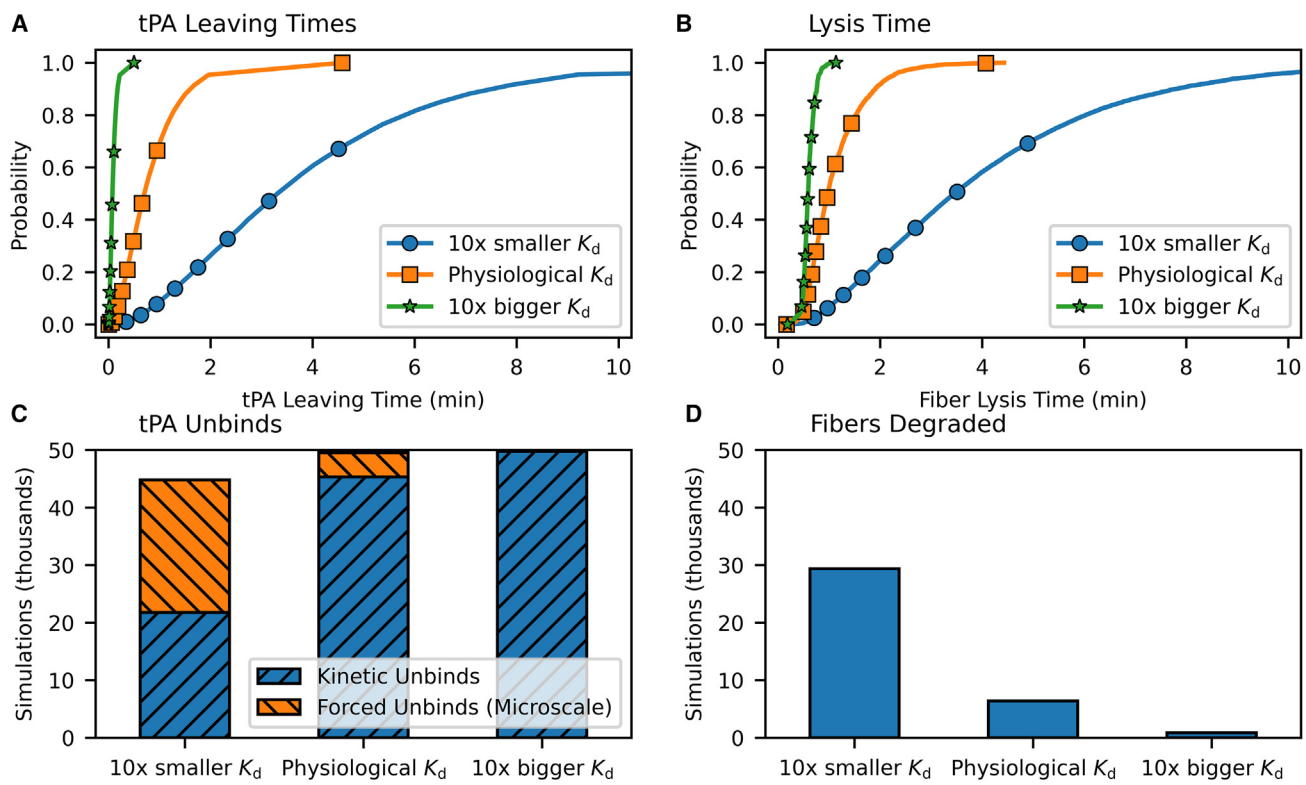


**FIGURE 3** Microscale model results. “10× smaller” corresponds to  $K_d = 0.036$  for tPA in the absence of plasminogen and  $K_d = 0.002 \mu\text{M}$  for tPA in the presence of plasminogen. “Physiological  $K_d$ ” corresponds to  $K_d = 0.36 \mu\text{M}$  and  $K_d = 0.02 \mu\text{M}$ , whereas “10× bigger” corresponds to  $K_d = 3.6$  and  $K_d = 0.2 \mu\text{M}$ . (A) Empirical cumulative distribution function of the time (in minutes) that tPA left the simulation. (B) Empirical cumulative distribution function of the time (in minutes) that the fiber was cleaved. (C) Number of simulations (out of 50,000) in which tPA unbinds, separated by unbinding type. Bars do not go all the way to 50,000 because in some simulations tPA stays bound for the entire simulation and hence never unbinds. (D) Number of simulations (out of 50,000) in which the fiber was cleaved along the simulated cross section. Data from these plots are presented numerically in Table S2.

(Fig. 3 B; Table S2). This average lysis time is within the range of experimentally measured single-fiber lysis times (25,26). Only about 12% of simulations (6366 out of 50,000) result in a fiber being cleaved before all the tPA and plasmin unbind from the cross section and fibrinolysis halts (Fig. 3 D). This gets translated to the macroscale model via the empirical cumulative distribution function; only about 12% of macroscale tPA bindings will result in cleavage of the fiber, meaning that multiple tPA-binding events will usually be necessary for a fiber to degrade.

The forced unbinding probability, or the fraction of simulations in which tPA was forced to unbind, is about 0.085, indicating that tPA is unbinding kinetically much more frequently than it is forced to unbind (Fig. 3 C). These microscale model results are independent of the rebinding mechanisms outlined above, which are all implemented in the macroscale model. So, the empirical distributions for tPA leaving time and for lysis time derived from these microscale data will be the same in all four rebinding mechanisms. Microscale model data are provided in Table S2.

**TABLE 2** Model tPA parameters

Parameter	Physiological $K_d$	10× bigger $K_d$	10× smaller $K_d$
$k_{\text{on}} (\mu\text{M}^{-1} \text{s}^{-1})$	0.1	0.1	0.1
$k_{\text{off no plasminogen}} (\text{s}^{-1})$	0.036	0.36	0.0036
$k_{\text{off with plasminogen}} (\text{s}^{-1})$	0.002	0.02	0.0002

See Table S1 for additional parameter values. “Physiological  $K_d$ ” corresponds to  $K_d = 0.36 \mu\text{M}$  for tPA in the absence of plasminogen (23) and  $K_d = 0.02 \mu\text{M}$  for tPA in the presence of plasminogen (24). “10× bigger” corresponds to  $K_d = 3.6$  and  $K_d = 0.2 \mu\text{M}$ , and “10× smaller” corresponds to  $K_d = 0.036$  and  $K_d = 0.002 \mu\text{M}$ .

## Macroscale model

For each of the four rebinding mechanisms, we run 10 independent simulations of the macroscale model, the output of which is found in Figs. 4, S3, and S4. When using physiological  $K_d$  values for tPA binding to fibrin (Table 2), we find that lysis is fastest when tPA can diffuse into the clot (“diffuse into clot” in Fig. 4 A has front velocities of just under 12  $\mu\text{m}/\text{min}$ ). The hypothesis for why this mechanism results in faster lysis is that tPA is no longer confined to a narrow band at the clot front; tPA can diffuse farther into the clot, initiating lysis on more fibers. This is supported

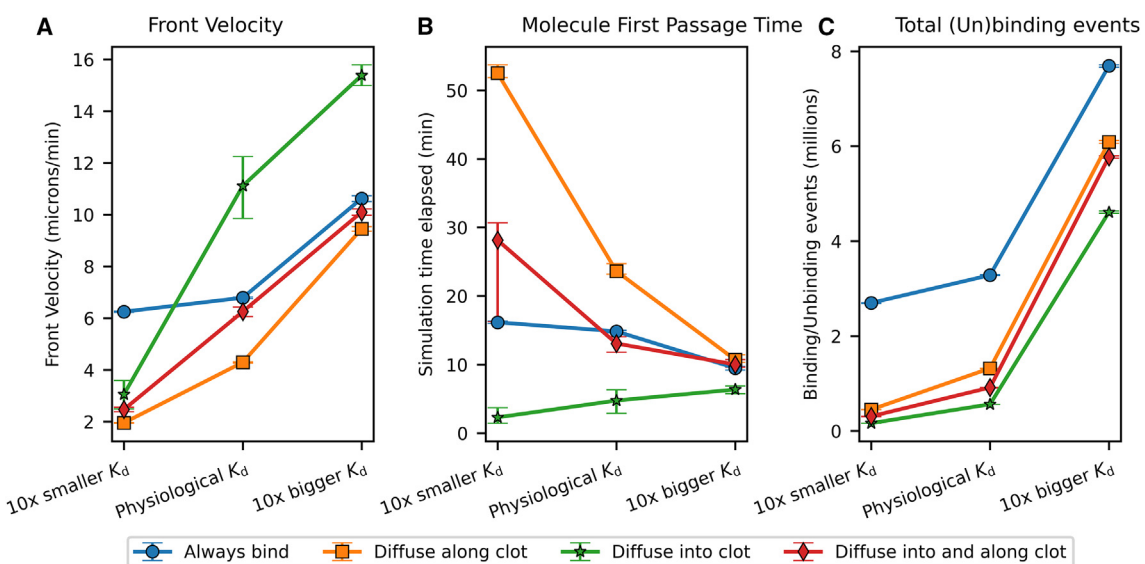


**FIGURE 4** Macroscale model results for the four unbinding mechanisms across three tPA variant scenarios. (A) Velocity of the degradation front. Lines show medians and error bars show interquartile ranges across 93  $x$ -locations across 10 independent simulations. (B) Time taken for tPA molecules to diffuse completely through the clot. Lines show medians and error bars show interquartile ranges across 43,074 molecules across 10 independent simulations. (C) Total number of molecule binding/unbinding events. Lines show means and error bars show minimum/maximum across 10 independent simulations.

by the large interquartile range (Fig. 4 A) for the diffuse-into-clot mechanism as it shows that some clot regions are degrading much faster than others. To verify this, we plot the position and state of fibrin and tPA at the point where 20% of fibers are degraded (Fig. 5). Indeed, we see that, in the diffuse-into-clot case, tPA (green and cyan) has diffused farther into the clot, causing degradation throughout the clot. Meanwhile the other three mechanisms all show bound tPA being concentrated at the degradation front, especially with the always-bind mechanism.

To quantify the effect the different mechanisms have on the diffusion of tPA, we calculate the first-passage time of tPA to reach the back edge of the clot. In one macroscale model simulation, we record the first time at which each of the 43,074 tPA molecules reaches the back edge of the clot. Then we average over the total number of molecules that do reach the back edge and call this value the mean first-passage time. Results show that tPA diffuses all the way through the clot about three-times faster in the diffuse-into-clot mechanism compared to the always-rebind and diffuse-into-and-along-clot mechanisms, whereas the diffuse-along-clot mechanism is almost two-times slower again (Fig. 4 B; Table S5). This faster diffusion of tPA through the clot is what drives the faster lysis front velocities (Fig. 4 A). The count of total binding events shows that mechanisms that include forced unbinding required fewer total binding events to fully degrade the clot (Fig. 4 C). A plot showing the proportion of tPA unbinding events of each type (kinetic, microscale forced, macroscale forced) for the different mechanisms is shown in Fig. 6. Recall that microscale forced unbinding occurs in the microscale model when plasmin degrades the binding doublet to which tPA is bound, whereas macroscale

forced unbinding occurs when plasmin degrades the fiber to which tPA is bound. When considering the proportion of unbinding events of each type (Fig. 6), it is not surprising that microscale forced unbinds are a constant fraction, since their probability of selection is fixed, based on the results of the microscale model. Macroscale forced unbinds happen when multiple tPA molecules bind to the same fiber in the macroscale model. It is therefore reasonable to deduce that the higher proportion of forced unbinds seen in the diffuse-along-clot and diffuse-into-and-along-clot mechanisms are the result of a higher number of tPA molecules concentrated at the lysis front, a feature that is less pronounced in the diffuse-into-clot mechanism.

### Confocal microscopy

To visualize the location of tPA during fibrinolysis and to support modeling predictions, experiments are performed with a fluorescently labeled fibrin clot and fluorescently labeled tPA (Fig. 7). Lysis did not qualitatively begin until 1.5 h after tPA delivery. Initially, tPA is largely present in the fibrin-free region or clustered along the clot edge (Fig. 7 A). Although difficult to observe with a merged image of fibrin and tPA, when the tPA channel is split from the clot, faint fibrin fiber features can be identified, which we attribute to the coating of some fibrin fibers with tPA molecules (Fig. 7 B). Time lapses reveal that these tPA molecules bind and unbind along the fibrin fibers closest to the clot edge as the bulk tPA diffuses into the clot to bind to fibers. Interestingly, the width of the tPA-coated fibrin clot region (Fig. 7 C) does not appear to change over the course of the 10-min time lapse. Lysis front position is measured over time (Fig. 7 D), relative to the time

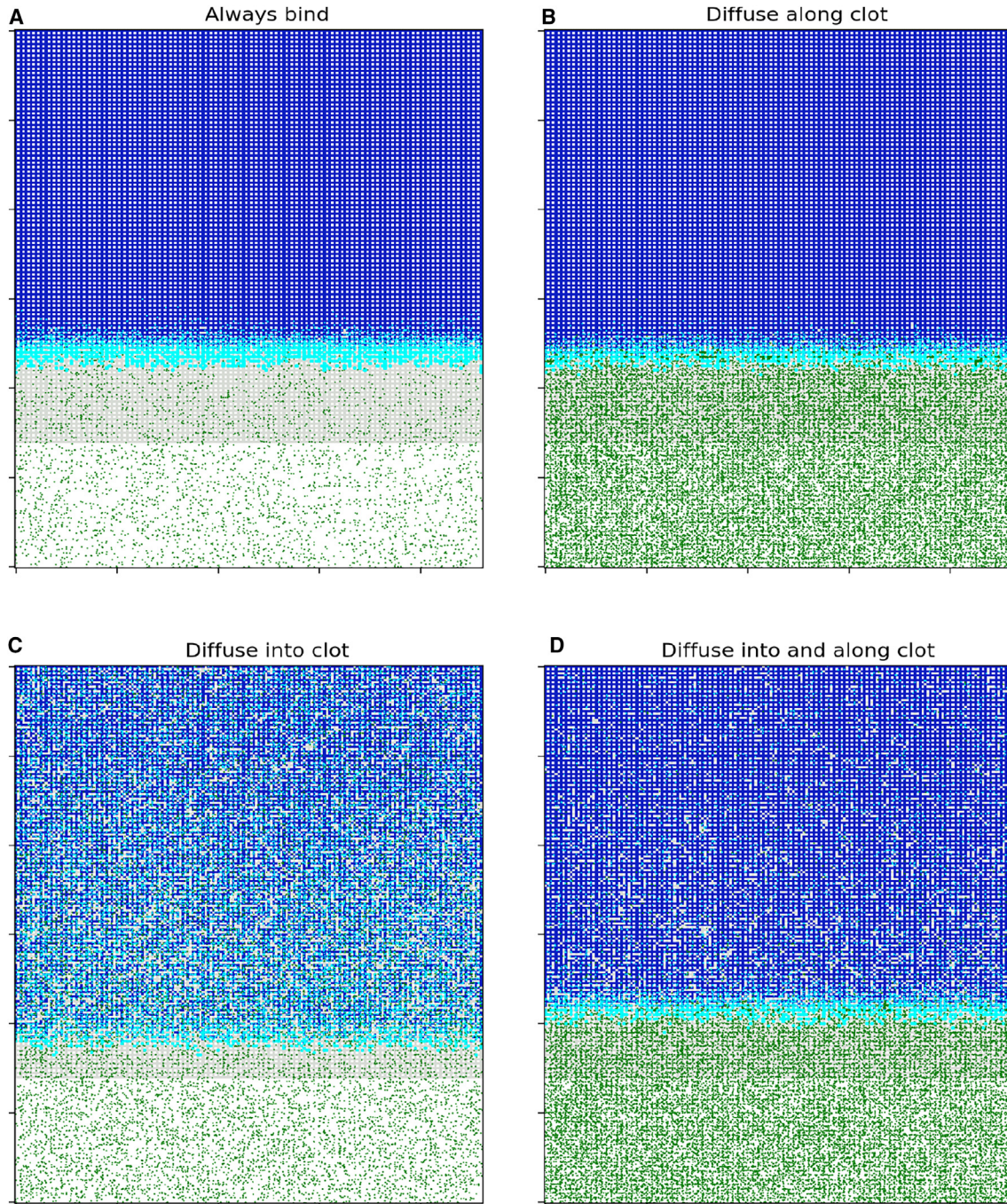
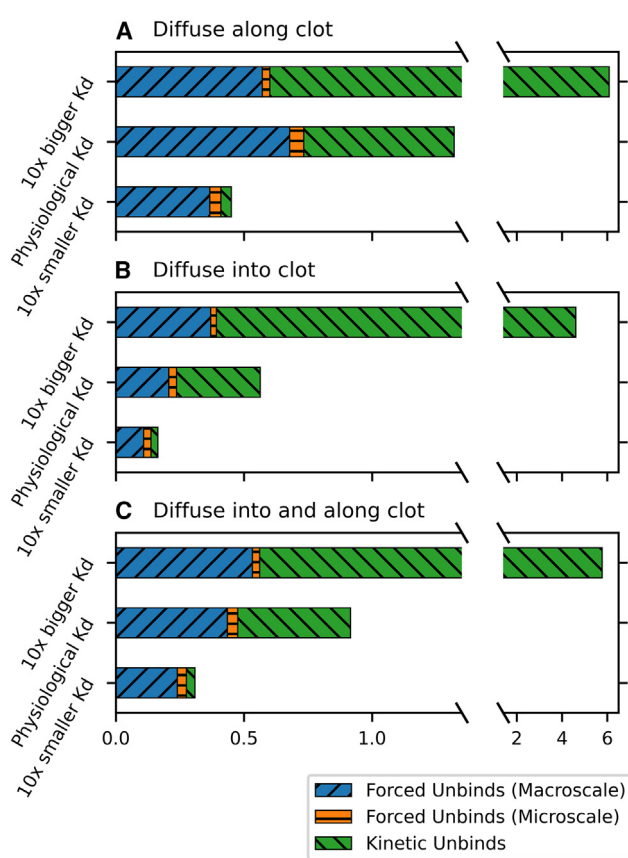


FIGURE 5 Macroscale clot and tPA for four mechanisms with physiological  $K_d$  at the point when 20% of fibers are degraded. All clots are  $10,862.67 \mu\text{m}^3$ . Undegraded fibrin is shown in blue, degraded fibrin in gray, bound tPA in cyan, and unbound tPA in green. All clots started at the same size and with the same amount of tPA. (A) Always rebind after 190 s. (B) Diffuse along clot after 260 s. (C) Diffuse into clot after 130 s. (D) Diffuse into and along clot after 200 s. Longer times to reach 20% degradation correspond to slower lysis rates.

since time-lapse capture of lysis began, rather than to time after initial delivery of tPA. Lysis did not begin immediately after tPA delivery (Video S1); in some experiments, lysis was first observed 1.5 h after tPA delivery. Video S2 shows a lysing clot.

Since the model predicts that lysis is fastest if tPA can diffuse into the clot bound to small FDPs, we perform exper-

iments with two abutting clots formed from different fluorescently labeled fibrinogen to test whether it is possible for FDPs to diffuse into the clot. Labeled tPA is added to initiate lysis, and time-lapse images are taken. Initially, there are two distinct clot regions corresponding to the two different clots: a top clot (blue) and a bottom clot (magenta) (Fig. 8 A). Labeled tPA is added to the edge of



**FIGURE 6** Proportion of tPA unbinding events by type for unbinding mechanisms. Diffuse along clot (**A**), diffuse into clot (**B**), and diffuse into and along clot (**C**), across three tPA variant scenarios. Results shown are means across 10 independent simulations. Total unbinding events here match those in **Fig. 4 C**. Note that results for the always-bind mechanism are not displayed since it considers all unbinding events to be kinetic.

the bottom clot. As the bottom clot lyses, there remains a fairly sharp distinction between the two clots (**Fig. 8 B**) for some time, but, eventually, fibrin from the bottom clot can be seen in the top clot region (**Fig. 8 C**, **Video S3**), indicating that FDPs from the bottom clot have diffused into the top clot. To further probe this observation, we measure the percentage area fraction over time of the region originally occupied by the top clot, which is composed of fluorophores from each clot (**Fig. 8 D**). Initially, there are virtually no bottom-clot (magenta) fluorophores in that region, but, as time goes on and the bottom clot starts to lyse, more than 50% of the top-clot region is composed of bottom-clot fluorophores. The percentage area fraction of top-clot fluorophores stays roughly constant around 100% until the tPA and FDPs diffuse into the region, at which point the top clot starts to lyse and the percentage area fraction therefore decreases.

### tPA variants

To test the effect of potential therapeutics that behave like tPA but have a different binding affinity to fibrin, we rerun

the computational experiments with tPA-like molecules that have a 10-times-bigger-than-physiological  $K_d$  and again with tPA-like molecules that have a 10-times-smaller-than-physiological  $K_d$  (see **Table 2** for parameter values). We find that a 10-times-smaller  $K_d$  results in a slower lysis front velocity in all mechanisms (**Fig. 4 A**; **Table S4**). The tPA variant stays bound to a single fiber for 134 s, on average, compared to 28 s for physiological  $K_d$  (**Fig. 3 A**; **Table S2**). Because the tPA variant is bound more strongly to fibrin, it is sequestered and unable to start degradation on other fibers, and it is also more likely to be forced to unbind by plasmin. This is reflected in the forced unbinding probability, which is over 0.5 (**Fig. 3 C**). Interestingly, when lysis is initiated with a tPA variant with a 10-times-smaller  $K_d$ , the lysis front velocity is fastest in the always-rebind mechanism, not the two diffuse-into-clot mechanisms (**Fig. 4 A**). This is likely because of the high probability of forced unbinding coupled with the strong binding affinity to fibrin. If the tPA variant is forced to unbind and can immediately rebind to another fiber and start the lytic process, lysis will happen faster than if tPA that is forced to unbind remains bound to a small piece of fibrin. In the latter case, because the kinetic unbinding rate is so slow, the tPA molecule is sequestered on fibrin and unable to initiate lysis on other fibers, as shown by the much smaller number of total binding events (**Fig. 4 C**).

A tPA variant with a 10-times-smaller  $K_d$  binds more strongly than physiological tPA to fibrin. In a mechanism where tPA is bound to small pieces of fibrin that can diffuse through the clot, this results in faster first-passage times (**Fig. 4 B**, diffuse-into-clot mechanism). This is because the tPA variant stays bound to the small piece of fibrin for a longer period of time, effectively hitching a ride farther into the clot. The tPA is not unbinding and then rebinding to a fiber as quickly as in the physiological  $K_d$  case, so it traverses a farther distance in the same amount of time. The first-passage times are slower for always-rebind, diffuse-along-clot, and diffuse-into-and-along-clot mechanisms because the tPA variant binds more strongly to fibrin and is unable to diffuse farther into the clot until it unbinds (unlike the diffuse-into-clot mechanism, where diffusion into the clot is happening even when the tPA is bound to small pieces of fibrin that have been cleaved from the clot). The slower first-passage times of the diffuse-into-and-along-clot mechanism might seem surprising, since it also allows the diffusion of small FDPs through the clot, but this only applies to molecules forced to unbind at the microscale level, which is a much smaller proportion of the total unbinding events (**Fig. 6 C**). We see only slightly slower first-passage times for the always-rebind mechanism compared to the physiological  $K_d$  case because the only slow down is coming from kinetic unbinding (**Fig. 4 B**). When tPA is forced to unbind in this mechanism, it is immediately available for diffusion and rebinding. In contrast, the first-passage times for the diffuse-along-clot mechanism are

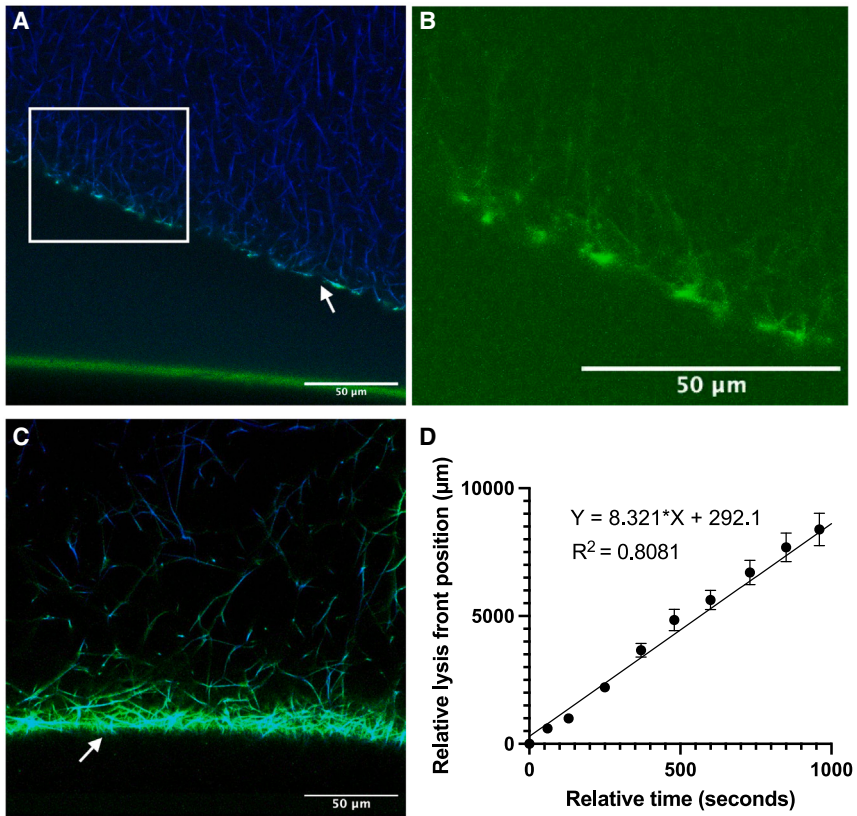


FIGURE 7 Experimental monitoring of fibrin clot degradation initiated by tPA. (A) Snapshot of a fibrin clot (blue) that is to be degraded by tPA (green). (B) A cropped and brightened snapshot of the tPA-only channel in the region outlined by the white box in (A). tPA molecules coating the fibrin fibers along the lysis front are visible. (C) Alternate view of clot after onset of lysis. Fibrin is shown in blue, tPA in green, and the overlap of fibrin and tPA in teal. (D) Lysis front position over time at 40× ( $n = 9$ ). Data points are plotted as mean  $\pm$  SE of the mean. A line was fitted with  $R^2 = 0.81$ . The white arrows in (A) and (C) denote the lysis front.

much higher in the 10-times-smaller  $K_d$  case compared to the physiological  $K_d$  case, because, when tPA is forced to unbind, it stays strongly bound to the FDP and is unable to diffuse farther into the clot. Snapshots comparing the clot and spatial distribution of tPA or tPA variants for the diffuse-into-and-along-clot mechanism are provided in Fig. S5. Snapshots for all mechanisms and  $K_d$  values are given in Figs. S6–S8.

For a 10-times-bigger-than-physiological  $K_d$ , the tPA variant kinetically unbinds from fibrin very quickly (Fig. 3 A), so it is forced to unbind by plasmin only rarely (the forced unbinding probability is 0.0054; Fig. 3 C). Because the tPA variant unbinds quickly, it can diffuse and rebind elsewhere quickly, too, effectively starting lysis on more fibers and resulting in faster lysis front velocities in all four mechanisms (Fig. 4 A). Another consequence of the lower rate of forced unbinding is fewer tPA molecules being bound to small pieces of cleaved fibrin and/or FDPs, and those that are quickly kinetically unbind. This results in shorter first-passage times in the diffuse-along-clot, diffuse-into-and-along-clot, and always-rebind mechanisms, because the weaker binding of the tPA variant allows deeper penetration of tPA into the clot. Interestingly, the first-passage times in the diffuse-into-clot mechanism with the 10-times-larger  $K_d$  tPA mutant are longer than its physiological tPA counterpart. In this mechanism, the weaker binding of the tPA variant

actually hinders the penetration of the tPA variant into the clot by releasing it from the small pieces of cleaved fibrin before it has diffused very far. Once released, it is likely to bind to a nearby part of the fibrin matrix, effectively stopping its diffusion until it is either forced to unbind or itunbinds kinetically.

## DISCUSSION

Despite much experimental and clinical work about the role of tPA in fibrinolysis, basic knowledge about the interplay between the functions of plasmin and tPA is lacking. Here, we investigate the effects of plasmin-mediated degradation of fibrin on the effective diffusion of tPA and the rate of fibrinolysis. By using a stochastic multiscale mathematical model to study four different possible mechanisms of tPA release from a fibrin clot, we show how important the plasmin-mediated unbinding of tPA can be, and we predict experimentally testable outcomes. We propose forced unbinding to be distinct from the standard kinetic unbinding of tPA (which is driven by the dissociation constant); forced unbinding occurs when plasmin degrades fibrin to which tPA is bound, releasing from the bulk clot a small fibrin fragment containing tPA. The tPA remains bound to the piece of fibrin (or FDP) until it kinetically unbinds sometime later. In the meantime, however, the movement of the tPA is dictated

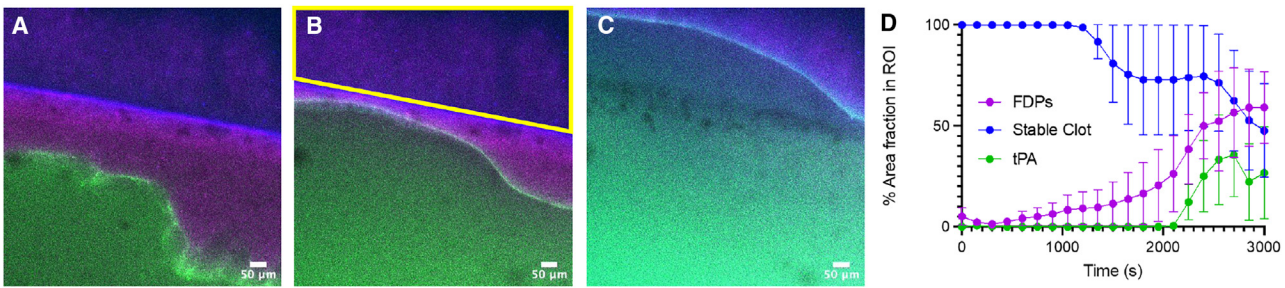


FIGURE 8 Experimental evidence for FDPs diffusing into the clot. (A–C) Time lapse of lysis of a fibrin network composed of two clots: top clot (Alexa Fluorophore 594, blue) and bottom clot (Alexa Fluorophore 647, magenta). Overlap between the two fluorophores appears in purple. Labeled tPA (488, green) is added to the bottom edge of the bottom clot. Yellow border in (B) outlines the area originally occupied by the top clot. This is the region of interest (ROI). Time points are at 0 s (A), 1440 s (B), and 3600 s (C). (D) Plot of the % area fraction of the ROI that is fibrin from the top clot (blue, stable clot), fibrin from the bottom clot (magenta, FDPs), and tPA (green) as a function of time.  $n = 3$ . Data is plotted as mean  $\pm$  SE mean.

by the fibrin fragment to which it is bound. We consider three possibilities: 1) the fibrin to which tPA is bound is small enough to diffuse freely throughout the clot (diffuse into clot); 2) the fibrin to which tPA is bound is large and unable to diffuse into the clot (diffuse along clot); 3) a combination of the first two (diffuse into and along clot). These three forced unbinding mechanisms are compared to a fourth baseline case in which all unbindings are considered to be kinetic (always rebind).

Our modeling shows that plasmin can either increase or decrease the effective diffusion of tPA through a fibrin clot, depending on the mechanism of tPA release from fibrin (Fig. 4 B and C). If tPA that is forced to unbind by plasmin remains bound to a small piece of fibrin that can diffuse into the clot, or is immediately available for rebinding, then plasmin increases the effective diffusion of tPA by releasing it from the clot sooner than it would have been released by kinetic unbinding alone. If, however, tPA that is forced to unbind by plasmin remains bound to larger FDPs that can only diffuse along or away from the clot, then plasmin decreases the effective diffusion of tPA by moving it farther away from the clot. As seen in the diffuse-into-clot and diffuse-into-and-along-clot mechanisms, plasmin-mediated forced unbinding of tPA enhances the effective diffusion of tPA by allowing it to hitch a ride farther into the clot than it would have by standard diffusion alone. Free tPA binds strongly to fibrin, so its diffusion into the clot is interrupted by binding; the result is a lot of tPA bound to a thin region of the clot front (6). If, however, tPA that was forced to unbind from the fiber remains bound to a small piece of fibrin, it can diffuse farther into the clot and then bind to a fiber farther from the front (once it kinetically unbinds from the piece of fibrin), thereby starting lysis on more fibers.

Lysis front velocity is also affected by the mechanism of tPA release from fibrin. Lysis is fastest in the diffuse-into-clot mechanism, followed by always rebind, diffuse into and along clot, and finally, at a much lower rate, diffuse along clot (Fig. 4 A). Since none of the kinetic parameters were varied between these simulations, the differences are

strictly due to the mechanism of tPA release. The effective diffusion of tPA through the clot (Fig. 4 B) along with snapshots of the fibrin and tPA distributions during lysis (Fig. 5) help explain why lysis is faster when every forced tPA unbinding results in tPA being bound to a small FDP that can diffuse through the clot. In that case, tPA is distributed much more uniformly throughout the clot region rather than being restricted to a thin region at the clot front, and therefore starts lysis on more fibers.

We hypothesize that the most likely mechanism for tPA release from the clot is the diffuse-into-and-along-clot mechanism. In this mechanism, tPA can kinetically unbind (in which case it is immediately available for rebinding) and be forced to unbind by plasmin-mediated degradation of fibrin. If plasmin degrades fibrin locally to the tPA binding site, it is conceivable that tPA could remain bound to a small FDP and be able to diffuse through the pores in the fibrin clot. If plasmin degrades a fibrin fiber on a more global scale, any tPA molecules bound to that fiber could conceivably be bound to larger FDPs that are too big to diffuse through the clot pores. If this is the mechanism of tPA release from fibrin clots, then our modeling suggests a novel positive feedback loop in the fibrinolytic process: the presence of plasmin enhances the diffusion of tPA, which consequently increases the lysis rate.

Experimental results support the model-derived hypothesis. By forming two clots with different fluorescent labels in such a way that the clots abut, we are able to measure the percentage area fraction of fluorophores in specific clot regions as lysis progresses. Since fluorescent fragments from one clot, along with tPA molecules, are recorded in the region occupied by the other clot (Fig. 8), we see that it is possible for small FDPs to diffuse into the clot. Further, when tracking the lysis front with labeled tPA (Fig. 7 B), tPA is seen to coat the fibrin fibers at the clot edge. However, lysis front movement does not occur immediately. The delay in lysis front progression (and therefore, effective tPA diffusion) further supports the idea that movement of tPA is dictated by the fibrin fragment to which it is bound. Initially, tPA is bound to full fibrin fibers or large FDPs that bind to

the remaining clot with an affinity proportional to their size. This confines tPA to a narrow band at the clot front. After tPA unbinds and initiates cleavage enough times that a significant number of smaller FDPs form, the smaller FDPs allow tPA to hitch a ride and diffuse through the clot pores. Since lysis of an experimental clot proceeds as a front with a high concentration of tPA at the front (Fig. 7), we conclude that diffuse into and along is a more likely mechanism than diffuse into (which showed less front-like lysis and a wider distribution of tPA in the model; Fig. 5).

Our experimental data indicate that FDPs can diffuse into the clot, but whether or not there exist FDPs that are too big to diffuse into the clot is an open question. The largest FDPs measured by Walker and Nesheim (16) should still be smaller than the 1- to 4- $\mu\text{m}$  pores in the clot, but their methods were unable to distinguish between FDPs bigger than  $2.5 \times 10^6$  Da. More likely, it is the case that larger FDPs are restricted from diffusing into the clot because they bind to the clot front; Walker and Nesheim suggest that larger FDPs bind to the remaining clot with a higher affinity than smaller FDPs bind to the clot (16). We suspect that the effect of large FDPs binding to the clot would be similar to the effect of large FDPs only being able to diffuse along the clot; in both scenarios, tPA is not able to hitch a ride farther into the clot. The binding of large FDPs to the intact fibrin, as well as the breakdown of large FDPs into smaller FDPs that diffuse into the clot, is something that can be investigated in the future. Additionally, we plan to use modeling and experiments to quantitatively measure the penetration of FDPs into the clot over time.

The work presented in this paper has implications for the development of new therapeutics. In particular, our work suggests investigating a tPA variant that behaves like tPA except with a weaker binding affinity to fibrin. Experiments of tPA mutants with a longer half-life, more resistance to inhibitors, and stronger binding affinities for fibrin have been conducted (12,13), but to our knowledge there has not been a similarly thorough study involving mutants with weaker binding affinities. One paper shows tPA variant reteplase, which has a reduced fibrin binding affinity, is a more efficacious fibrinolytic agent than tPA (14), consistent with our model predictions. Our models suggest that a fibrin clot will be lysed faster if initiated by a tPA variant with a 10-times-bigger-than-physiological  $K_d$ , regardless of the mechanism underlying forced tPA unbinding. Importantly, if the true mechanism of forced tPA unbinding is like our diffuse-into-clot mechanism, then using a tPA variant with a bigger  $K_d$  actually slows down the diffusion of tPA through the clot (Fig. 4 B), which might help minimize the systemic bleeding issues common in stroke patients. Even with the diffuse-into-and-along-clot mechanism, the first-passage times of the 10-times-bigger tPA variant through the clot are not much different from physiological tPA, so it is possible that using a variant with a larger  $K_d$  could accel-

erate lysis but not make systemic bleeding complications worse than they currently are. In the future, we plan to repeat the experimental studies in this paper with other degradation agents, such as tenecteplase and reteplase, to test the model hypothesis that a larger  $K_d$  will result in faster lysis.

## CONCLUSIONS

We proposed a novel mechanism influencing fibrinolysis: the forced unbinding of tPA from fibrin via plasmin-mediated fibrin degradation. By modifying an existing stochastic multiscale model of fibrinolysis, we showed that forced unbinding of tPA affects the effective diffusion of tPA through the clot and how quickly the clot degrades. Using a combination of modeling and laboratory experiments, we hypothesized that tPA is released from clots via what we call a diffuse-into-and-along mechanism. We propose that sometimes the forced-unbound tPA is on small FDPs that can diffuse freely through the clot, whereas other times it is on larger FDPs that are only able to diffuse along or away from the clot. Due to the effects of forced unbinding, a tPA variant with a weaker binding affinity to fibrin (i.e., a larger  $K_d$ ) could be a worthwhile target for improved stroke treatment. We showed that a tPA variant with a 10-times-larger  $K_d$  degrades a clot faster than regular tPA, without significantly increasing the effective diffusion of enzyme through the clot (which is important to minimize systemic bleeding). This work highlights the power of mathematical modeling, which can be used to propose and test biological mechanisms. Coupling the modeling to laboratory experimentation increases the benefit of each and creates insights that may have been impossible from modeling or experiments alone.

## SUPPORTING MATERIAL

Supporting material can be found online at <https://doi.org/10.1016/j.bpj.2024.02.002>.

## AUTHOR CONTRIBUTIONS

B.E.B. designed, carried out, and interpreted results from the modeling studies. B.P. ran model simulations, collected model data, and made visualizations of all results. R.R. and V.T. designed laboratory experiments. R.R. and M.S. ran laboratory experiments and, along with V.T., interpreted results. The manuscript was written by B.E.B. and B.P. with contributions from R.R., M.S., and V.T.

## ACKNOWLEDGMENTS

The authors gratefully acknowledge the following funding sources: NIH R00HL148646-01 (V.T.); New Jersey Commission on Cancer Research COCR22PRF010 (R.A.R.); NIH T32 GM135141 (R.A.R.); and New Jersey Commission on Spinal Cord Research CSCR23IRG005 (V.T.). B.E.B. gratefully acknowledges the University of Central Oklahoma CURE-STEM

Bannish et al.

Scholars program and the Buddy high performance computing resources (NSF Major Research Instrumentation #1429702).

## DECLARATION OF INTERESTS

The authors declare no competing interests.

## REFERENCES

1. Weisel, J. W., and R. I. Litvinov. 2017. Fibrin Formation, Structure and Properties. *Subcell. Biochem.* 82:405–456.
2. Weisel, J. W., and R. I. Litvinov. 2013. Mechanisms of Fibrin Polymerization and Clinical Implications. *Blood.* 121:1712–1719.
3. Risman, R. A., N. C. Kirby, ..., V. Tutowler. 2023. Fibrinolysis: an illustrated review. *Res. Pract. Thromb. Haemost.* 7, 100081. <https://www.sciencedirect.com/science/article/pii/S2475037923000493>.
4. Henschen, A., and J. McDonagh. 1986. Fibrinogen, fibrin and factor XIII. *N. Compr. Biochem.* 13:171–241.
5. GBD 2016 Neurology Collaborators. 2019. Global, regional, and national burden of neurological disorders, 1990–2016: a systematic analysis for the Global Burden of Disease Study 2016. *Lancet Neurol.* 18:459–480.
6. Longstaff, C., C. Thelwell, ..., K. Kolev. 2011. The interplay between tissue plasminogen activator domains and fibrin structures in the regulation of fibrinolysis: kinetic and microscopic studies. *Blood.* 117:661–668.
7. Sakharov, D. V., J. F. Nagelkerke, and D. C. Rijken. 1996. Rearrangements of the Fibrin Network and Spatial Distribution of Fibrinolytic Components during Plasma Clot Lysis. *J. Biol. Chem.* 271:2133–2138.
8. Collet, J. P., D. Park, ..., J. W. Weisel. 2000. Influence of Fibrin Network Conformation and Fibrin Fiber Diameter on Fibrinolysis Speed : Dynamic and Structural Approaches by Confocal Microscopy. *Arterioscler. Thromb. Vasc. Biol.* 20:1354–1361.
9. Staessens, S., F. Denorme, ..., S. F. De Meyer. 2020. Structural analysis of ischemic stroke thrombi: histological indications for therapy resistance. *Haematologica.* 105:498–507. <http://www.haematologica.org/content/105/2/498>.
10. Saver, J. L. 2004. Number Needed to Treat Estimates Incorporating Effects Over the Entire Range of Clinical Outcomes: Novel Derivation Method and Application to Thrombolytic Therapy for Acute Stroke. *Arch. Neurol.* 61:1066–1070. <https://doi.org/10.1001/archneur.61.7.1066>.
11. Chapman, S. N., P. Mehendiratta, ..., A. M. Southerland. 2014. Current perspectives on the use of intravenous recombinant tissue plasminogen activator (tPA) for treatment of acute ischemic stroke. *Vasc. Health Risk Manag.* 10:75–87.
12. Klegerman, M. E. 2017. Translational initiatives in thrombolytic therapy. *Front. Med.* 11:1–19.
13. Khasa, Y. P. 2017. The evolution of recombinant thrombolytics: Current status and future directions. *Bioengineered.* 8:331–358.
14. Martin, U., U. Kohnert, ..., S. Fischer. 1996. Comparison of the recombinant Escherichia coli-produced protease domain of tissue-type plasminogen activator with alteplase, reteplase and streptokinase in a canine model of coronary artery thrombolysis. *Thromb. Haemostasis.* 76:1096–1101.
15. National Institute of Neurological Disorders and Stroke. 2023. Tissue Plasminogen Activator for Acute Ischemic Stroke (Alteplase, Activase). U.S. Department of Health and Human Services, National Institutes of Health, Retrieved July 13, 2023 from. <https://www.ninds.nih.gov/about-ninds/impact/ninds-contributions-approved-therapies/tissue-plasminogen-activator-acute-ischemic-stroke-alteplase-activaser>.
16. Walker, J. B., and M. E. Nesheim. 1999. The Molecular Weights, Mass Distribution, Chain Composition, and Structure of Soluble Fibrin Degradation Products Released from a Fibrin Clot Perfused with Plasmin. *J. Biol. Chem.* 274:5201–5212.
17. Bannish, B. E., I. N. Chernysh, ..., J. W. Weisel. 2017. Molecular and Physical Mechanisms of Fibrinolysis and Thrombolysis from Mathematical Modeling and Experiments. *Sci. Rep.* 7:6914.
18. Bannish, B. E., J. P. Keener, and A. L. Fogelson. 2014. Modelling fibrinolysis: a 3D stochastic multiscale model. *Math. Med. Biol.* 31:17–44. <https://doi.org/10.1093/imammb/dqs029>. Epub 2012.
19. Gillespie, D. T. 1976. A General Method for Numerically Simulating the Stochastic Time Evolution of Coupled Chemical Reactions. *J. Comput. Phys.* 22:403–434.
20. Gillespie, D. T. 1977. Exact Stochastic Simulation of Coupled Chemical Reactions. *J. Phys. Chem.* 81:2340–2361.
21. Li, W., J. Sigley, ..., M. Guthold. 2016. Fibrin Fiber Stiffness Is Strongly Affected by Fiber Diameter, but Not by Fibrinogen Glycation. *Biophys. J.* 110:1400–1410. <https://doi.org/10.1016/j.bpj.2016.02.021>.
22. Collet, J. P., C. Lesty, ..., J. W. Weisel. 2003. Dynamic Changes of Fibrin Architecture during Fibrin Formation and Intrinsic Fibrinolysis of Fibrin-rich Clots. *J. Biol. Chem.* 278:21331–21335.
23. Horrevoets, A., A. Smilde, ..., H. Pannekoek. 1994. The Specific Role of Finger and Kringle 2 Domains of Tissue-type Plasminogen Activator during *in vitro* Fibrinolysis. *J. Biol. Chem.* 269:12639–12644.
24. Bachmann, F. 1994. The plasminogen-plasmin enzyme system. In *Hemostasis and Thrombosis: Basic Principles and Clinical Practice*, Third edition. R. W. Coleman, J. Hirsh, and V. J. Marder, eds Philadelphia: J. B. Lippincott Company, pp. 1592–1622.
25. Cone, S. J., A. T. Fuquay, ..., N. E. Hudson. 2020. Inherent fibrin fiber tension propels mechanisms of network clearance during fibrinolysis. *Acta Biomater.* 107:164–177. <https://doi.org/10.1016/j.actbio.2020.02.025>.
26. Lynch, S. R., S. M. Laverty, ..., N. E. Hudson. 2022. Microscale structural changes of individual fibrin fibers during fibrinolysis. *Acta Biomater.* 141:114–122. <https://doi.org/10.1016/j.actbio.2022.01.006>.

**Supplemental information**

**The effect of plasmin-mediated degradation on fibrinolysis and tissue plasminogen activator diffusion**

**Brittany E. Bannish, Bradley Paynter, Rebecca A. Risman, Mitali Shroff, and Valerie Tutwiler**

## MODELING AND EXPERIMENTAL SET-UP

Parameter values used in the model are given in Supplementary Table 1. The diffusion coefficient,  $50 \mu\text{m}^2/\text{s}$ , is characteristic for small molecules and was taken from Diamond and Anand (1). Based on the Stokes-Einstein equation with  $T = 310 \text{ K}$  (body temperature) and  $\eta = 1.257 \text{ mPa}\cdot\text{s}$  (viscosity of blood plasma at body temperature), this diffusion coefficient corresponds to a spherical particle with radius  $\sim 3.6 \text{ nm}$ . Erickson provides an estimate for the minimum radius of a sphere that could contain the given mass of a protein (2). Their minimum radius ranges from 2.4-3.05 nm for a protein of mass 50-100 kDa (tPA is 68 kDa), on the same order of magnitude as the radius given by Stokes-Einstein for our diffusion coefficient. Thus, it is reasonable to model tPA diffusion with this diffusion coefficient.

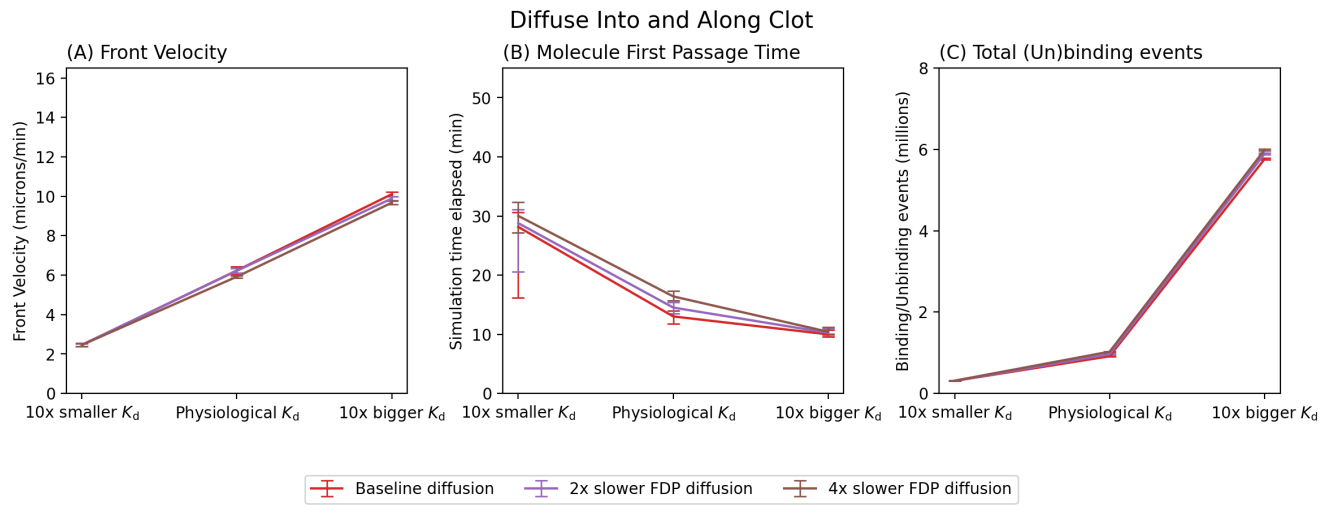
Supplementary Table 1: Parameters for computational models. “Physiological  $K_d$ ” corresponds to  $K_d = 0.36 \mu\text{M}$  for tPA in the absence of plasminogen and  $K_d = 0.02 \mu\text{M}$  for tPA in the presence of plasminogen. “10-times bigger  $K_d$ ” corresponds to  $K_d = 3.6$  and  $K_d = 0.2 \mu\text{M}$ , and “10-times smaller  $K_d$ ” corresponds to  $K_d = 0.036$  and  $K_d = 0.002 \mu\text{M}$ . Plasmin is abbreviated “PLi” and plasminogen is abbreviated “PLG”.

Parameter	Physiological $K_d$	10-times bigger $K_d$	10-times smaller $K_d$
tPA binding rate to fibrin ( $\mu\text{M}^{-1}\text{s}^{-1}$ )	0.1	0.1	0.1
tPA unbinding rate from fibrin with no plasminogen ( $\text{s}^{-1}$ )	0.036	0.36	0.0036
tPA unbinding rate from fibrin with plasminogen ( $\text{s}^{-1}$ )	0.002	0.02	0.0002
PLi-mediated rate of fibrin degradation ( $\text{s}^{-1}$ )	5	5	5
Concentration of free plasminogen ( $\mu\text{M}$ )	2	2	2
PLG unbinding rate from intact fibrin ( $\text{s}^{-1}$ )	3.8	3.8	3.8
PLG unbinding rate from nicked fibrin ( $\text{s}^{-1}$ )	0.22	0.22	0.22
PLG binding rate to fibrin ( $\mu\text{M}^{-1}\text{s}^{-1}$ )	0.1	0.1	0.1
PLi unbinding rate from fibrin ( $\text{s}^{-1}$ )	57.6	57.6	57.6
tPA-mediated rate of conversion of PLG to PLi ( $\text{s}^{-1}$ )	0.1	0.1	0.1
PLi-mediated rate of exposure of new binding sites ( $\text{s}^{-1}$ )	5	5	5
Clot volume ( $\mu\text{m}^3$ )	10,862.67	10,862.67	10,862.67
Pore size ( $\mu\text{m}$ )	1.0135	1.0135	1.0135
Fiber diameter ( $\mu\text{m}$ )	0.0727	0.0727	0.0727
Total fibers	25,761	25,761	25,761
tPA molecules	43,074	43,074	43,074
Diffusion coefficient ( $\mu\text{m}^2\text{s}^{-1}$ )	50	50	50
Moving probability	0.2	0.2	0.2
Time step (ms)	0.3424	0.3424	0.3424

We use the same diffusion coefficient for tPA and FDPs, even though the diffusion coefficient would depend on the molecular weight and shape of the particle. Small FDPs (50-200 kDa (3)) are on the same order of magnitude as tPA (68 kDa), and therefore can reasonably be treated as diffusing similarly to tPA, if molecular weight is the only consideration. However, Walker and Nesheim find that small FDPs behave approximately like rigid rods (3). Experimental work comparing the diffusion coefficients of spherical and rod-like particles found that the spheres diffused 3.8-times faster than the rods (4), however, the rods had a molecular weight that was 7-times greater than the molecular weight of the spheres, so it's not clear how much of the difference in diffusion coefficients was due to shape vs size. To test whether slower diffusion of small FDPs would qualitatively change our model results, we reran the “into and along” scenarios with 2- or 4-times slower diffusion of small FDPs. Model results changed negligibly (Supplementary Figure 1). Larger FDPs could also be modeled with slower diffusion coefficients, but this would only accentuate the slower lysis and mean first passage times that we already see, so for simplicity we chose to keep the diffusion coefficient constant for all diffusing quantities.

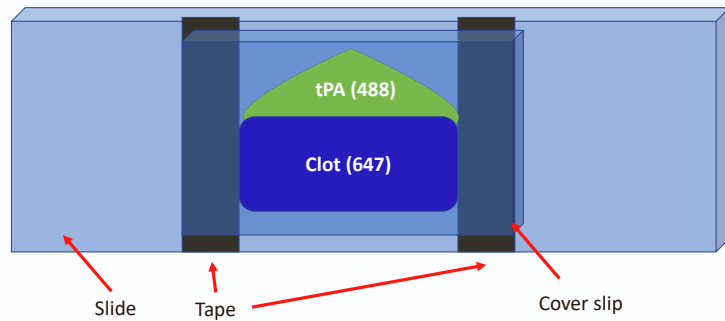
We also assume that free tPA diffusion is unhindered by the fibrin clot. The pore size of the model clot ( $1.0135 \mu\text{m}$ ) is about 3 orders of magnitude bigger than the size of tPA (approximately 3 nm in radius), and fibrin accounts for less than 20% of the clot volume, so it is reasonable to model tPA using unhindered diffusion. Additionally, it has been shown experimentally that over a physiologically relevant range of fibrinogen concentrations (inclusive of our concentration), fibrin networks do not form a strong diffusion barrier and minimally restrict diffusion of thrombin (5), a molecule on the same order of magnitude as tPA.

The three laboratory experiments were set up as shown in Supplementary Figure 2.

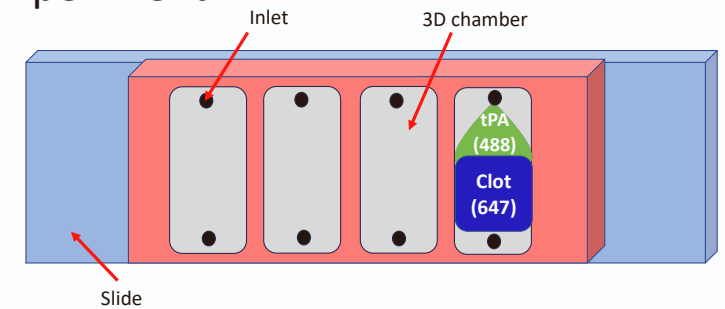


Supplementary Figure 1: The effect of different FDP diffusion rates on the “Diffuse into and along clot” mechanism. Note that the red plots here are identical to the corresponding plots on Figure 4. (A) Velocity of the degradation front. Lines show medians and error bars show interquartile ranges across 93-locations across ten independent simulations. (B) Time taken for tPA molecules to diffuse completely through the clot. Lines show medians and error bars show interquartile ranges across 43,074 molecules across ten independent simulations. (C) Total number of molecule binding/unbinding events. Lines show means and error bars show min/max across ten independent simulations.

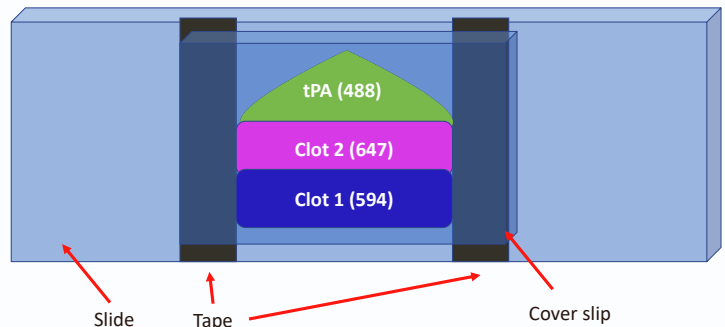
## Experiment 1



## Experiment 2



## Experiment 3



Supplementary Figure 2: Experimental design for the three laboratory experiments. 1) Chamber created with tape with one labeled clot and labeled tPA, 2) chamber from Electron Microscope labs with one labeled clot and labeled tPA, 3) chamber created with tape with two labeled clots and unlabeled tPA. Specific fluorophores used for each experiment are given in parentheses.

## ADDITIONAL DATA

Here we provide tables of data represented graphically in figures in the main text, as well as additional supporting figures.

Microscale model results for the three different dissociation constants are given in Supplementary Table 2. For each of the four rebinding mechanisms, we run 10 independent simulations of the macroscale model, the output of which is found in Supplementary Figure 3. It is notable that, although error bars for the minimum and maximum of the ten simulations are plotted, they are barely visible due to stability of the model. Comparing these curves we can see that the “diffuse into clot” mechanism causes much more rapid lysis, the “diffuse along clot” mechanism causes slower lysis, and the combination of the two mechanisms in “diffuse into and along clot” brings the degradation curve back towards the baseline “always bind” mechanism. These patterns can also be seen when isolating the degradation rate (Supplementary Figure 4D) and complete degradation time (Supplementary Figure 4C).

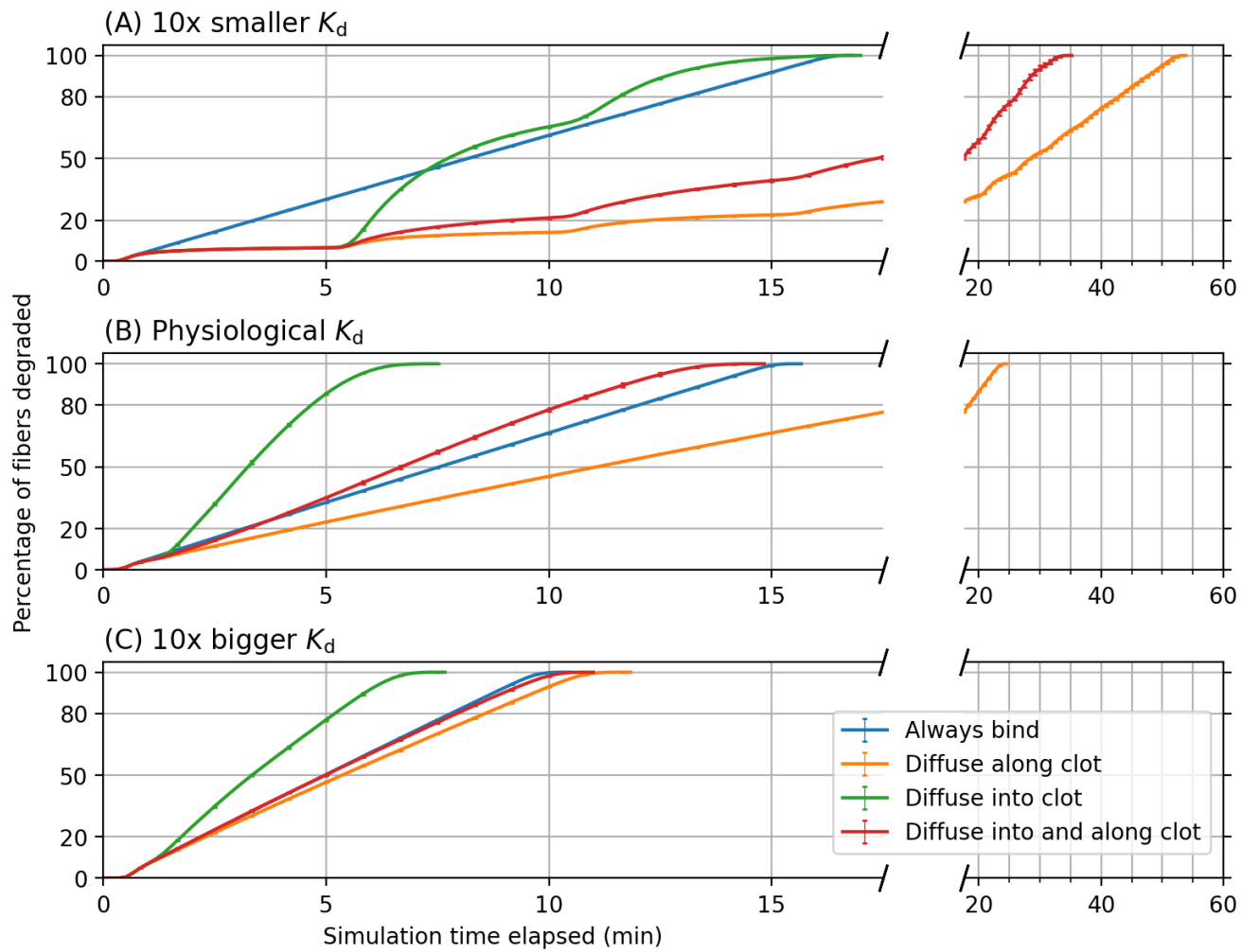
Macroscale model data for the four unbinding mechanisms and three different dissociation constants are provided in Supplementary Tables 3 – 6.

Supplementary Table 2: Microscale model results. “Physiological  $K_d$ ” corresponds to  $K_d = 0.36 \mu\text{M}$  for tPA in the absence of plasminogen and  $K_d = 0.02 \mu\text{M}$  for tPA in the presence of plasminogen. “10x bigger” corresponds to  $K_d = 3.6$  and  $K_d = 0.2 \mu\text{M}$ , and “10x smaller” corresponds to  $K_d = 0.036$  and  $K_d = 0.002 \mu\text{M}$ . “Fibers Degraded” gives the number of simulations (out of 50,000) for which the fiber was cleaved along the simulated plane. Lysis times are presented as mean  $\pm$  standard deviation for those fibers that degraded. “tPA Unbound” gives the number of simulations (out of 50,000) for which tPA was unbound from the simulated fiber. Results for tPA leaving time are presented as mean  $\pm$  standard deviation for those tPA that unbound. “tPA Forced to Unbind” is calculated as the percentage of simulations (out of 50,000) in which tPA was forced to unbind by plasmin-mediated degradation out of the total number of simulations (out of 50,000) in which tPA unbound (either kinetically or by force).

Scenario	Fibers Degraded	Lysis Time (s)	tPA Unbound	tPA Leaving Time (s)	tPA Forced to Unbind
Physiological $K_d$	6,366	$54.154 \pm 27.089$	49,529	$28.192 \pm 34.175$	8.52%
10x smaller $K_d$	29,357	$148.333 \pm 119.613$	44,783	$134.361 \pm 154.095$	51.43%
10x bigger $K_d$	838	$34.550 \pm 7.349$	50,000	$3.122 \pm 3.796$	0.54%

Supplementary Table 3: Macroscale clot degradation measures. Lag time is time to 5% degraded (in min), complete degradation is time to 100% degraded (in min) and degradation rate is the average slope between 20% and 80% degraded (in %/min). All data is presented as the mean  $\pm$  standard deviation of 10 independent simulations. “Physiological  $K_d$ ” corresponds to  $K_d = 0.36 \mu\text{M}$  for tPA in the absence of plasminogen and  $K_d = 0.02 \mu\text{M}$  for tPA in the presence of plasminogen. “10x bigger” corresponds to  $K_d = 3.6$  and  $K_d = 0.2 \mu\text{M}$ , and “10x smaller” corresponds to  $K_d = 0.036$  and  $K_d = 0.002 \mu\text{M}$ .

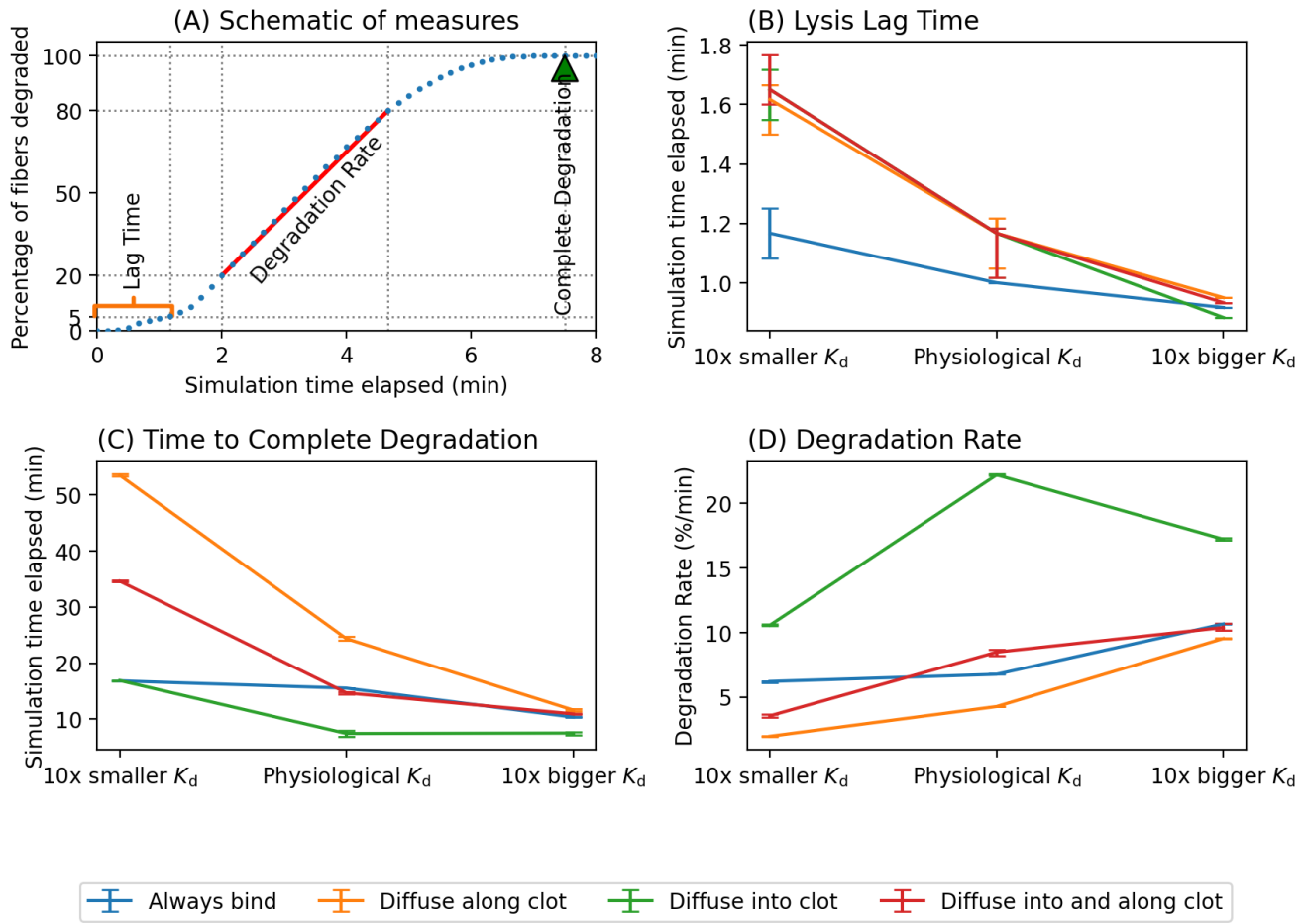
Measure	Mechanism	Physiological $K_d$	10x bigger $K_d$	10x smaller $K_d$
Lag Time (min)	Always bind	$1.00 \pm 0.00$	$0.92 \pm 0.08$	$1.17 \pm 0.00$
	Diffuse along clot	$1.17 \pm 0.00$	$0.95 \pm 0.08$	$1.62 \pm 0.08$
	Diffuse into clot	$1.17 \pm 0.00$	$0.88 \pm 0.08$	$1.65 \pm 0.05$
	Diffuse into and along clot	$1.17 \pm 0.00$	$0.93 \pm 0.08$	$1.65 \pm 0.05$
Complete Degradation Time (min)	Always bind	$15.53 \pm 0.07$	$10.37 \pm 0.07$	$16.83 \pm 0.00$
	Diffuse along clot	$24.33 \pm 0.07$	$11.63 \pm 0.10$	$53.43 \pm 0.17$
	Diffuse into clot	$7.45 \pm 0.08$	$7.53 \pm 0.07$	$16.88 \pm 0.11$
	Diffuse into and along clot	$14.68 \pm 0.16$	$10.95 \pm 0.08$	$34.58 \pm 0.39$
Degradation Rate (%/min)	Always bind	$6.77 \pm 0.02$	$10.67 \pm 0.03$	$6.21 \pm 0.02$
	Diffuse along clot	$4.27 \pm 0.01$	$9.54 \pm 0.03$	$1.96 \pm 0.01$
	Diffuse into clot	$22.22 \pm 0.19$	$17.23 \pm 0.07$	$10.58 \pm 0.20$
	Diffuse into and along clot	$8.48 \pm 0.07$	$10.39 \pm 0.04$	$3.55 \pm 0.03$



Supplementary Figure 3: Percentage of clot degraded for four unbinding mechanisms across three tPA variant scenarios. Ten simulations of each were run with lines showing the means and error bars showing the range of values measured.

Supplementary Table 4: Lysis front velocity. Lysis front velocity is measured in  $\mu\text{m}/\text{min}$  and is presented as the mean  $\pm$  standard deviation of 10 independent simulations. “Physiological  $K_d$ ” corresponds to  $K_d = 0.36 \mu\text{M}$  for tPA in the absence of plasminogen and  $K_d = 0.02 \mu\text{M}$  for tPA in the presence of plasminogen. “10x bigger” corresponds to  $K_d = 3.6$  and  $K_d = 0.2 \mu\text{M}$ , and “10x smaller” corresponds to  $K_d = 0.036$  and  $K_d = 0.002 \mu\text{M}$ .

Mechanism	Physiological $K_d$	10x bigger $K_d$	10x smaller $K_d$
Always bind	$6.78 \pm 0.05$	$10.62 \pm 0.16$	$6.25 \pm 0.04$
Diffuse along clot	$4.29 \pm 0.04$	$9.45 \pm 0.15$	$1.95 \pm 0.02$
Diffuse into clot	$11.00 \pm 1.83$	$15.39 \pm 0.59$	$3.07 \pm 0.76$
Diffuse into and along clot	$6.25 \pm 0.27$	$10.10 \pm 0.19$	$2.47 \pm 0.13$



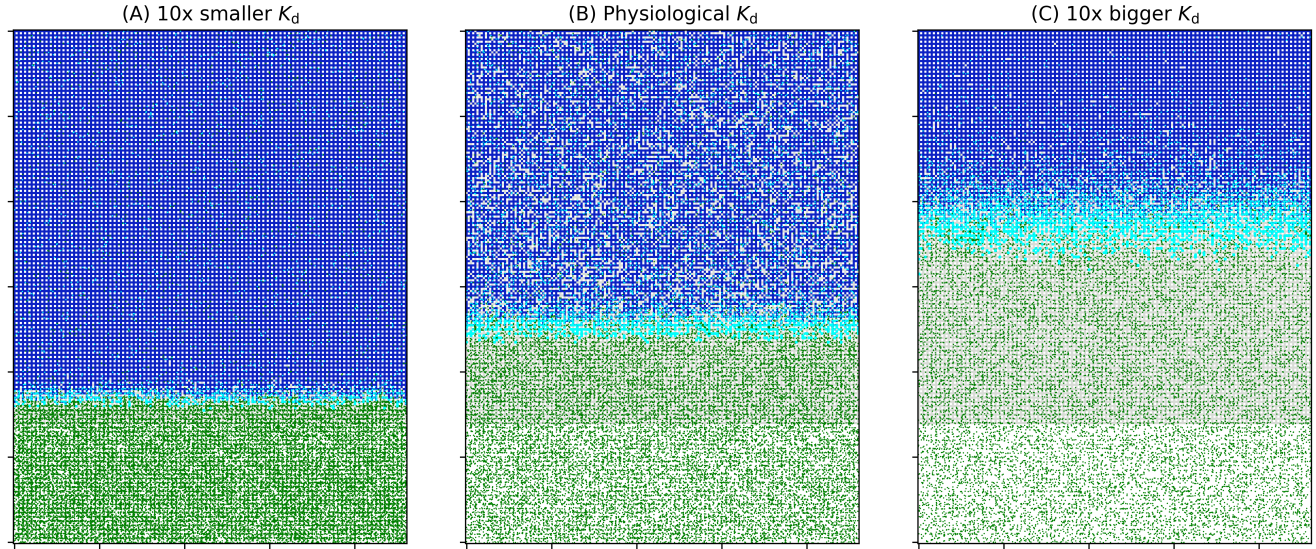
Supplementary Figure 4: Measures of overall degradation for the macroscale model. (A) A schematic diagram showing how these measures are calculated. These are: lysis lag time at 5% degradation (B), complete degradation time at 100% degradation (C), and degradation rate as the slope between 20% and 80% degradation (D). For (B-D) lines show means and error bars show min/max across ten independent simulations.

Supplementary Table 5: Mean first passage time for tPA to reach the back edge of the clot. Mean first passage time is measured in minutes and is presented as the mean  $\pm$  standard deviation across 10 independent simulations. Means are calculated using only the tPA molecules that make it to the back edge of the clot during the simulation. For all mechanisms and all choices of  $K_d$ , at least 95% of the 43,074 tPA molecules make it to the back of the clot.

Mechanism	Physiological $K_d$	10x bigger $K_d$	10x smaller $K_d$
Always rebind	$14.90 \pm 0.52$	$9.61 \pm 0.76$	$16.22 \pm 0.48$
Diffuse along clot	$24.07 \pm 1.32$	$11.03 \pm 1.17$	$52.92 \pm 1.45$
Diffuse into clot	$4.64 \pm 2.23$	$6.45 \pm 1.19$	$3.04 \pm 2.43$
Diffuse into and along clot	$12.34 \pm 3.21$	$10.27 \pm 1.26$	$23.27 \pm 10.09$

Supplementary Table 6: tPA binding and unbinding counts for the macroscale model. The total number of binding events in a simulation is equal to the total unbinding events in that simulation. “Forced Unbinds (Microscale)” are those unbinds in the macroscale model that are randomly chosen to be part of the fraction of tPA molecules whose binding sites were degraded by plasmin on the microscale level. “Forced Unbinds (Macroscale)” are those tPA molecules that were bound to a fiber at the time the fiber degraded at the macroscale level. All data is presented as the mean  $\pm$  standard deviation of 10 independent simulations. “Physiological  $K_d$ ” corresponds to  $K_d = 0.36 \mu\text{M}$  for tPA in the absence of plasminogen and  $K_d = 0.02 \mu\text{M}$  for tPA in the presence of plasminogen. “10x bigger” corresponds to  $K_d = 3.6$  and  $K_d = 0.2 \mu\text{M}$ , and “10x smaller” corresponds to  $K_d = 0.036$  and  $K_d = 0.002 \mu\text{M}$ .

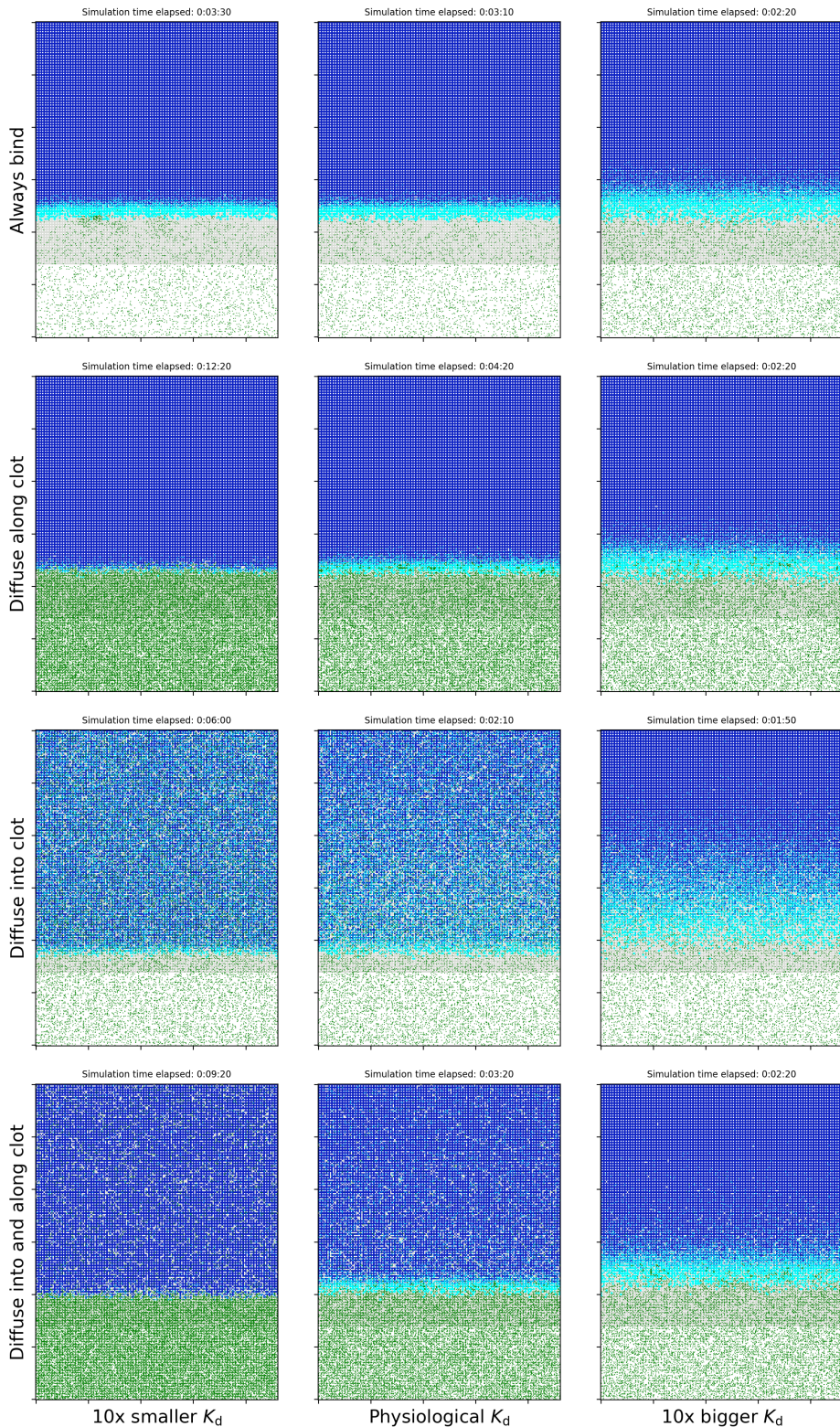
Measure	Mechanism	Physiological $K_d$	10x bigger $K_d$	10x smaller $K_d$
(Un)binds	Always bind	$3,282,330 \pm 5,383$	$7,691,678 \pm 17,160$	$2,697,297 \pm 4,987$
	Diffuse along clot	$1,319,787 \pm 2,495$	$6,087,131 \pm 19,143$	$450,483 \pm 1,258$
	Diffuse into clot	$563,173 \pm 1,029$	$4,607,247 \pm 14,444$	$163,973 \pm 747$
	Diffuse into and along clot	$915,270 \pm 3,506$	$5,771,655 \pm 16,160$	$308,601 \pm 1,993$
Forced Unbinds (Microscale)	Always bind	N/A	N/A	N/A
	Diffuse along clot	$54,698 \pm 238$	$29,825 \pm 138$	$43,483 \pm 227$
	Diffuse into clot	$30,523 \pm 258$	$22,928 \pm 198$	$28,778 \pm 161$
	Diffuse into and along clot	$40,968 \pm 131$	$28,150 \pm 152$	$35,459 \pm 194$
Forced Unbinds (Macroscale)	Always bind	N/A	N/A	N/A
	Diffuse along clot	$678,033 \pm 1,022$	$571,187 \pm 1,077$	$365,964 \pm 1,026$
	Diffuse into clot	$206,027 \pm 803$	$369,515 \pm 583$	$107,985 \pm 528$
	Diffuse into and along clot	$434,868 \pm 2,193$	$532,955 \pm 725$	$239,593 \pm 1,924$



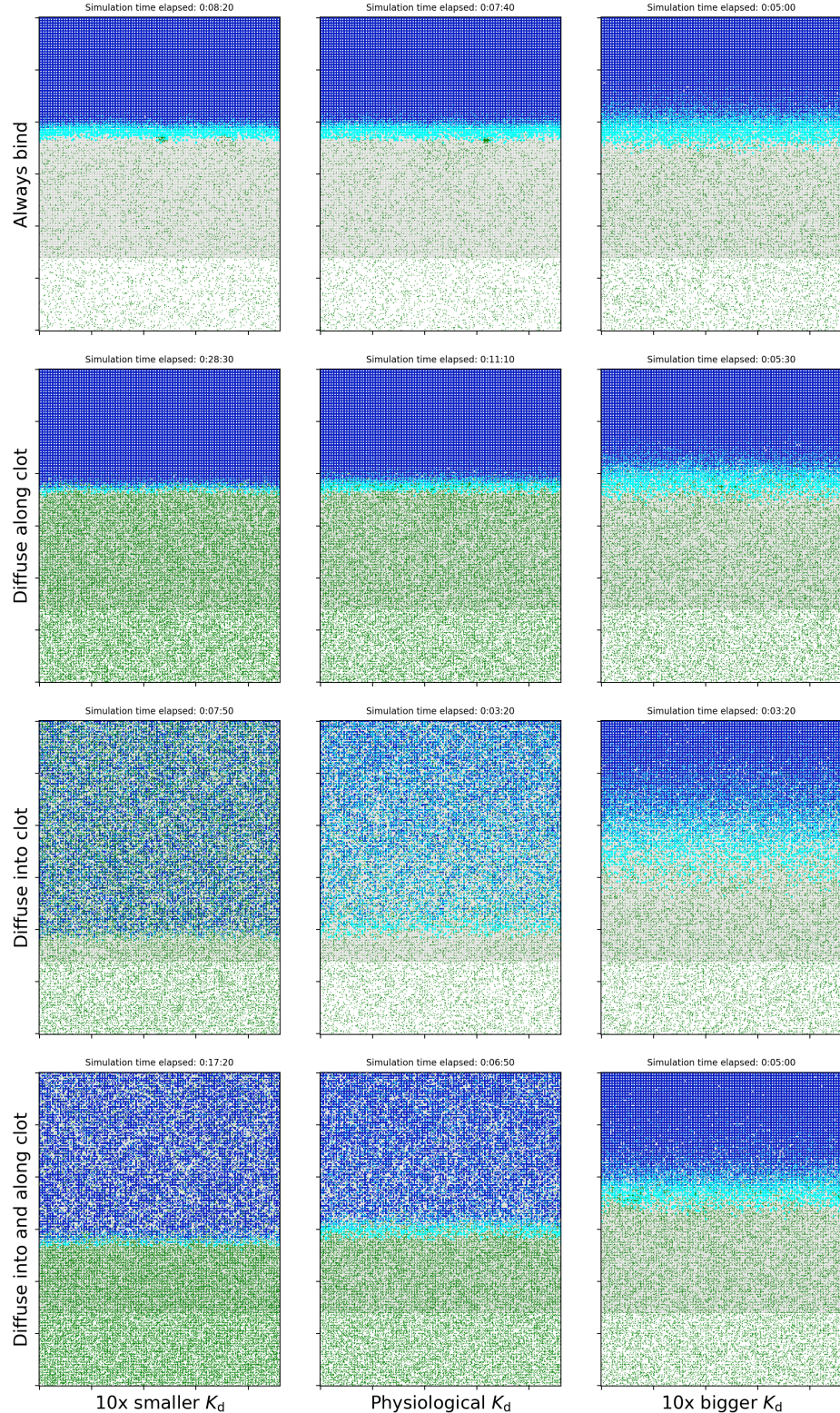
Supplementary Figure 5: Macroscale clot and bound tPA for the ‘Diffuse into and along clot’ mechanism for three tPA variant scenarios, 5 minutes after tPA was added. Undegraded fibrin is shown in blue, degraded fibrin gray, bound tPA cyan, and unbound tPA is shown in green. All clots started at the same size, and with the same amount of tPA. (A) 10 times smaller  $K_d$  (6.6% degraded). (B) Physiological  $K_d$  (34.9% degraded). (C) 10 times bigger  $K_d$  (50.2% degraded). Simulation time elapsed given as h:mm:ss.

Snapshots of the model clot and tPA 5 minutes after introduction of tPA illustrate the differences between the three tPA variants for the “diffuse into and along clot” mechanism (Supplementary Figure 5). For the 10x-bigger variant, there is a wider band of bound tPA at the clot front and more of the clot has degraded compared to the physiological tPA case. For the 10x-smaller variant, bound tPA is constrained to a much narrower band at the clot front and fibrinolysis proceeds much more slowly.

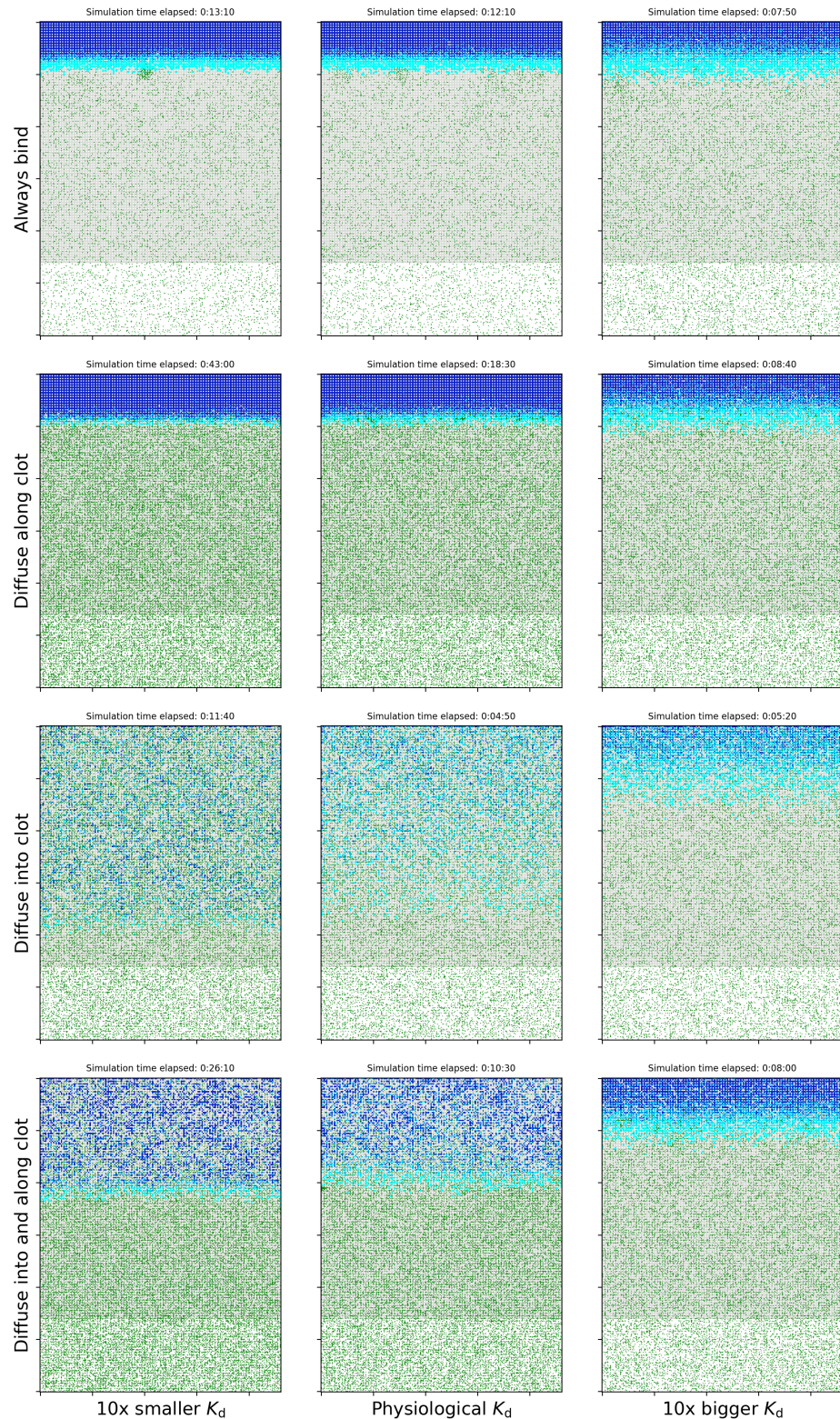
For completeness, snapshots of the model clot for all mechanisms and dissociation constants are shown when 20% of all fibers have degraded (Supplementary Figure 6), 50% of fibers have degraded (Supplementary Figure 7), and 80% of fibers have degraded (Supplementary Figure 8).



Supplementary Figure 6: Macroscale clot and bound tPA for all four mechanism for three tPA variant scenarios, after 20% degradation. Undegraded fibrin is shown in blue, degraded fibrin gray, bound tPA cyan, and unbound tPA is shown in green. All clots started at the same size, and with the same amount of tPA. Simulation time elapsed given as h:mm:ss.



Supplementary Figure 7: Macroscale clot and bound tPA for all four mechanism for three tPA variant scenarios, after 50% degradation. Undegraded fibrin is shown in blue, degraded fibrin gray, bound tPA cyan, and unbound tPA is shown in green. All clots started at the same size, and with the same amount of tPA. Simulation time elapsed given as h:mm:ss.



Supplementary Figure 8: Macroscale clot and bound tPA for all four mechanism for three tPA variant scenarios, after 80% degradation. Undegraded fibrin is shown in blue, degraded fibrin gray, bound tPA cyan, and unbound tPA is shown in green. All clots started at the same size, and with the same amount of tPA. Simulation time elapsed given as h:mm:ss.

Supplemental Video 1: No lysis occurs for 10 minutes after addition of tPA.

Supplemental Video 2: A lysing clot.

Supplemental Video 3: Lysis of two-clot system, showing FDPs from one clot diffusing into second clot.

## REFERENCES

1. Diamond, S. L., and S. Anand, 1993. Inner Clot Diffusion and Permeation during Fibrinolysis. *Biophysical Journal* 65:2622–2643.
2. Erickson, H. P., 2009. Size and Shape of Protein Molecules at the Nanometer Level Determined by Sedimentation, Gel Filtration, and Electron Microscopy. *Biological Procedures Online* Article number 32.
3. Walker, J. B., and M. E. Nesheim, 1999. The Molecular Weights, Mass Distribution, Chain Composition, and Structure of Soluble Fibrin Degradation Products Released from a Fibrin Clot Perfused with Plasmin. *The Journal of Biological Chemistry* 274:5201–5212.
4. Lee, K. L., L. C. Hubbard, S. Hern, I. Yildiz, M. Gratzl, and N. F. Steinmetz, 2013. Shape matters: the diffusion rates of TMV rods and CPMV icosahedrons in a spheroid model of extracellular matrix are distinct. *Biomaterials Science* 1:581–588.
5. Kim, O., Z. Xu, E. D. Rosen, and M. S. Alber, 2013. Fibrin Networks Regulate Protein Transport during Thrombus Development. *PLOS Computational Biology* 9(6):e1003095.